

Here is a sample chapter from
The Physics of Radiotherapy X-Rays and Electrons®.

This sample chapter is copyrighted and made available for personal use only. No part of this chapter may be reproduced or distributed in any form or by any means without the prior written permission of Medical Physics Publishing.

You can order this book in one of two formats:

Hardcover: ISBN 978-1-951134-10-5

eBook: ISBN 978-1-951134-11-2

To order by phone, call MPP at 1-800-442-5778
or visit medicalphysics.org.

Medical Linear Accelerators

“A boy surfing on a water wave provides a useful traveling wave analogy.”

—Karzmark and Morton, 2017

1.1 Introduction

For the treatment of deep-seated tumors, high-energy x-rays with penetrating characteristics are required. The medical linear accelerator (linac) is currently the most popular device for this application. To ensure a full understanding of linac beam properties, it is important to review the mechanism of x-ray beam production by these types of devices.

Early historically significant methods of producing x-ray beams for external beam radiotherapy (teletherapy) consisted of conventional x-ray tubes (with anode and cathode) producing x-rays of energy up to about 300 kV (Johns et al. 1952a). These superficial (up to 150 kV) and orthovoltage (up to 300 kV) machines are still used very effectively for treatment of skin cancer. They do not, however, provide skin-sparing properties (Locke et al. 2001), and their beams are not penetrating enough to treat deep-seated tumors effectively.

The search for a more penetrating beam led to the development of cobalt-60 machines (Johns et al. 1952b, 1959). These became more popular than other teletherapy sources (e.g., cesium-137) because a large source activity of several thousand Curies of cobalt-60 could be packed into very small cylinders with diameters of about 10 mm (Johns and Cunningham 1983). The cobalt-60 machine is still used in radiotherapy applications today. A cobalt-60 beam spectrum has two photopeaks, at 1.17 and 1.33 MeV, giving a mean photon energy of about 1.25 MeV. Despite their rather low photon energy compared with that of a linac, they still provide reasonable skin sparing properties, as maximum dose is achieved at a depth of 0.5 cm. Cobalt-60 units are very reliable due to their relatively simple design.

The evolution of the linac was a direct result of radar development work that culminated in the production of microwave generators in the form of magnetrons and the klystrons. The first reported use of a medical linac was in 1953 (Thwaites and Tuohy 2006), but due to cost and complexity leading to reliability issues, they coexisted with Cobalt-60 units in radiotherapy departments for decades. As reliability improved, linacs gained ascendancy in the 1980s, and they are currently the most frequently used modality for radiotherapy applications. By 2013 there were only 1880 cobalt-60 units in operation globally, compared with 11,000 linacs (Attun et al. 2015).

Linacs are capable of establishing intense electromagnetic fields in microwave cavities. This enables the acceleration of electrons to relativistic velocities when incorporated with suitable waveguide structures. In summary, linacs have the following important features:

1. Linacs have multiple electron and photon energies that allow the physician to tailor treatment to the required treatment depth. A modern linac is usually capable of producing at least two different photon energies and a number of different electron energies.
2. Linacs have relatively high dose rates (1 to 15 Gy per minute). This enables short treatment times.
3. Linacs have a sharp dose fall-off at the beam edge in the penumbra.

Currently the most compelling alternatives to using linac x-ray beams seems to be protons. Data from the Particle Therapy Co-operative Group (PTCOG) confirm there are currently about 60 clinical proton facilities worldwide with about 30 new centers currently under construction (PTCOG 2021). Building a synchrotron or cyclotron to produce protons is a high-cost option, even though the beam line may be shared by several (usually three) treatment delivery portals. The gantries may be on the order of 100 tons, and complex magnetic beam steering is required. The cost of these facilities varies, but the capital expenditure for such a facility is typically between 5 to 20 times more expensive than for setting up an x-ray linac facility. With the recent introduction of superconducting cyclotrons and smaller synchrotrons, single-room proton facilities are now available with capital costs being significantly lower than multi-room solutions.

Synchrotrons can also be used to deliver heavier particles, such as carbon-12. There are currently a handful of carbon-12 beam lines with associated gantries being used to treat cancer patients. Carbon-12 is particularly interesting, as it seems to have a direct ionizing damage effect (like neutrons) that makes it suitable for treating hypoxic tumors such as prostate (Ishikawa et al. 2006). Synchrotron designs exist that can combine beam lines to provide carbon-12 to one gantry and protons to another within the same facility.

One very favorable property of protons and carbon-12—which x-rays do not possess—is their well-defined Bragg peak. Due to this, the beam reaches a peak of dose deposition at significant depth and then has a rapid fall-off beyond this depth. Proton beams of 250 MeV are used to treat deep-seated tumors, and at about 90 MeV they play a role in treating optic melanomas. Historical randomized trials comparing protons with x-rays are limited (Shipley et al. 1995). Discussions of recent clinical trials in progress are outlined by Bekelman et al. (2018).

In this chapter the basic operational features of linacs are described in Section 1.2. More details of magnetrons, klystrons, and linac waveguides are described in sections 1.3 to 1.5. Beam delivery systems in the treatment head—including bend-

ing magnets, collimators, and beam-modifying devices—are described in sections 1.6 to 1.8. Gantry-mounted image guidance devices are introduced in Section 1.9, and innovative machines that utilize linac technology are introduced in Section 1.10.

1.2 Principles of Linac Operation

1.2.1 External and Geometric Features

Figure 1.1 shows photographs of the external features of two commonly used *open gantry* radiotherapy linacs. Common features of these linacs are:

1. The patient is placed on the treatment couch, which has vertical, horizontal, and rotational movements in the horizontal plane for patient positioning.
2. The linac beam production devices are mounted in the stand and gantry.
3. The stand is fixed and holds the gantry in position.
4. The gantry is able to rotate within a 360-degree arc around the patient to enable different beam angles to be aimed at the patient.
5. The collimators are internally mounted at the end of the gantry.
6. The size and angle of the collimators are also adjustable.

1.2.2 Operational Systems Overview

A detailed schematic showing a generic linac waveguide and beam path with beam monitoring and collimation systems is shown in Figure 1.2. This figure shows the main components of the linac that are housed in the gantry represented in a two-dimensional schematic. Figure 1.2a represents a linac with a bending magnet and carousel capable of x-ray and electron production. Figure 1.2b shows an in-line linac with a fixed target. These in-line configurations are common in closed gantry designs, such as the Varian Halcyon™, Ethos™, and the Accuray Tomotherapy™ machines (Pictures of these machines are shown at the end of this chapter.) Note that these in-line linacs have no bending magnet. The target is usually fixed to save space and reduce complexity (i.e., no carousel), so they do not have an electron mode.

The linac accelerates electrons linearly to high velocity and energy using high-power microwaves. The heart of the linac is the accelerating waveguide, where acceleration of electrons occurs. The microwave energy required to accelerate the electrons is delivered to the accelerating structure in the form of short-duration pulses (5 microseconds in duration) from the klystron or magnetron via a rectangular transmission microwave waveguide.

An electron gun injects low-energy electrons at one end of the accelerating waveguide. The timing of the electron injections into the guide is controlled by a gun driver system. The electrons are accelerated along the guide to speeds approaching the speed of light. The electrons then enter a bending magnet assembly where they are redirected toward the center of the beam's gantry axis of rotation, known as *isocenter*.

When a linac is operated in x-ray mode, the electron beam hits a target and x-rays are produced by the bremsstrahlung production process. When the linac is used in electron mode, the electrons generally strike a scattering foil prior to exiting the linac.

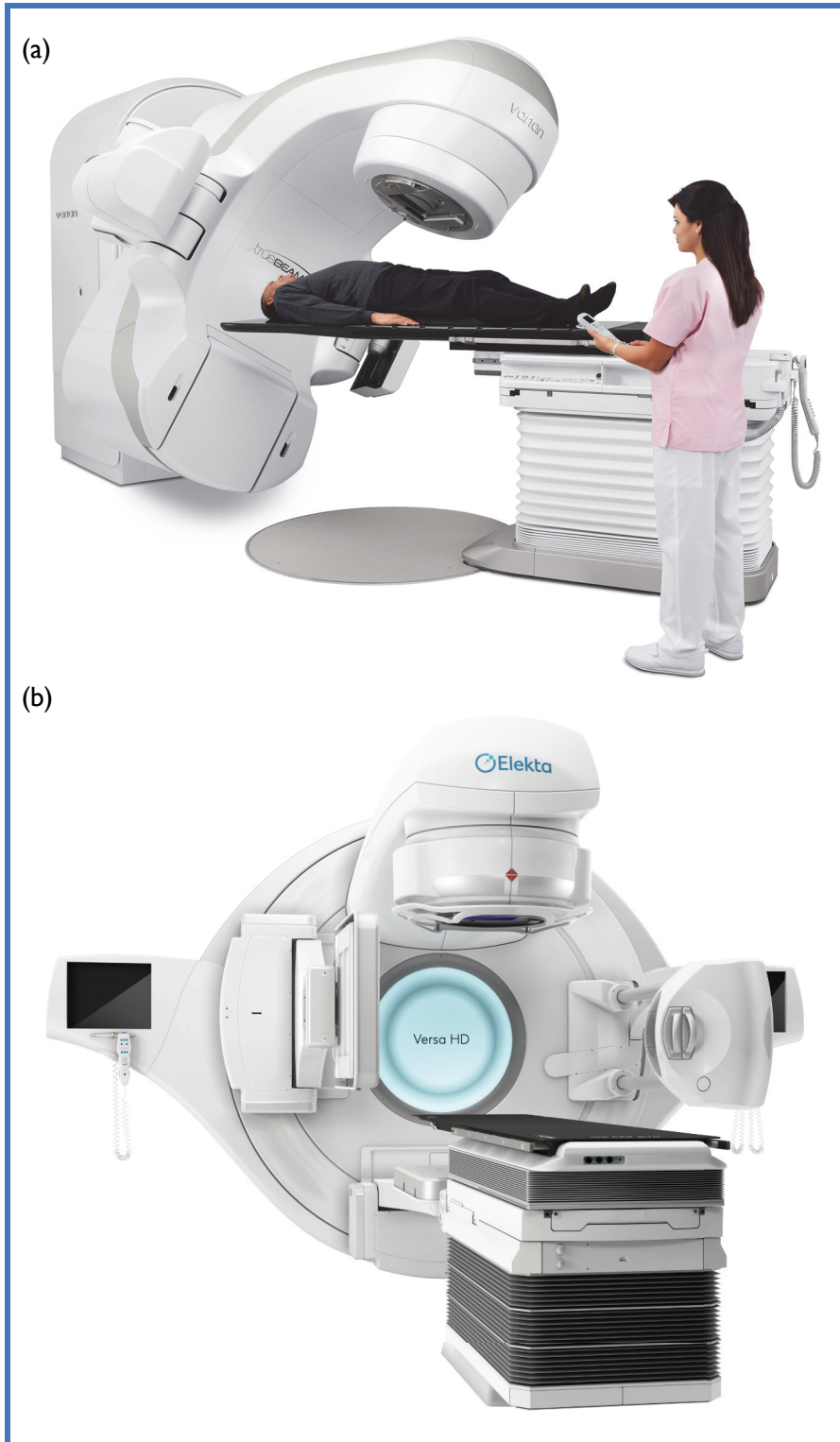


Figure 1.1 Medical linear accelerators (linacs). (a) Varian TrueBeam®. (Image courtesy of Varian Medical Systems, Inc. All rights reserved.) (b) Elekta Versa HD™ linac. (Image courtesy of Elekta.)

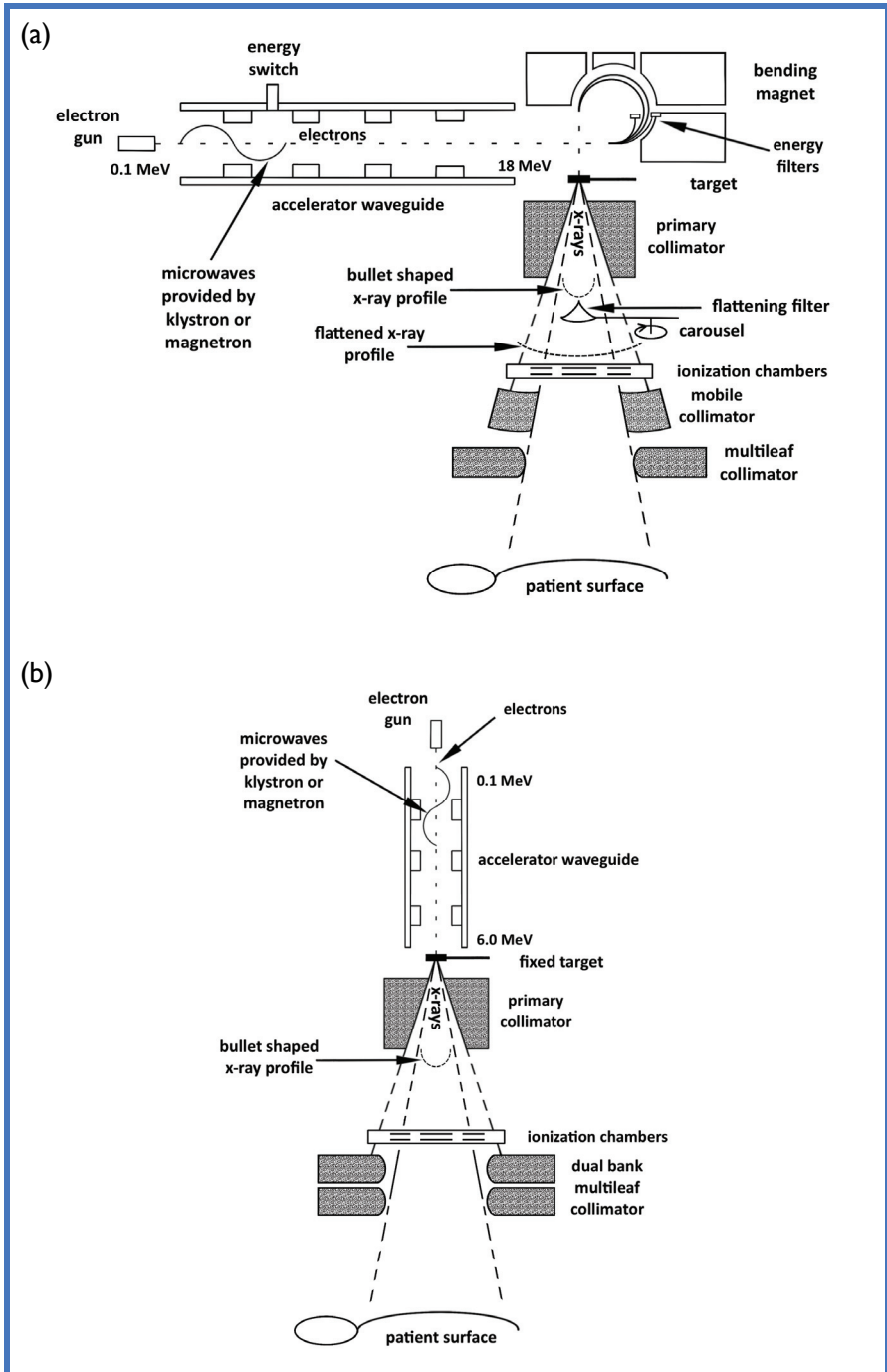


Figure 1.2

Linac guide configurations. (a) Linac beam horizontal guide delivery system schematic shown in two dimensions, including gun, guide, bending magnet, movable target, flattening filter, carousel to house electron foils, and collimation systems. These linacs usually have a removable target and are capable of producing multiple x-ray and electron energies up to about 23 MeV. (b) Linac beam vertical guide delivery system schematic shown in two dimensions, including gun, guide, target, and collimation systems. These linacs have a fixed target and do not have an electron mode. Modern designs also do not have a flattening filter and deliver one fixed x-ray energy, e.g., 6 MV.

Descriptions in this text are intended to give the reader an understanding of the principles of operation of the main components of the linac. Detailed descriptions of technical design variations of components—such as waveguide structures and bending magnets—can be obtained elsewhere (Podgorsak et al. 1999; Karzmark and Morton 2017).

1.2.3 Auxiliary Systems Overview

The other important component systems and auxiliary systems that are critical to linac function are shown in Figure 1.3. The auxiliary support systems of the linac as described by Greene (1986) consist of:

- a water-cooling system to regulate the temperature of linac components, e.g., the bending magnet;
- a vacuum ion pump system to provide vacuum for the accelerating waveguide;
- an air pressure system, as the target is driven by pneumatic air pressure; and
- a gas system to improve the dielectric strength of the transmission waveguide.

1.2.4 The Modulator

The modulator circuit supplies high-voltage pulses to the cathode of the microwave generator (e.g., klystron). To do this, a three-phase, full-wave rectifier and solid-state diodes are used to deliver about 10 kV to the *pulse forming network* (PFN). The PFN is an inductor/capacitor diode circuit that charges up and, when the hydro-

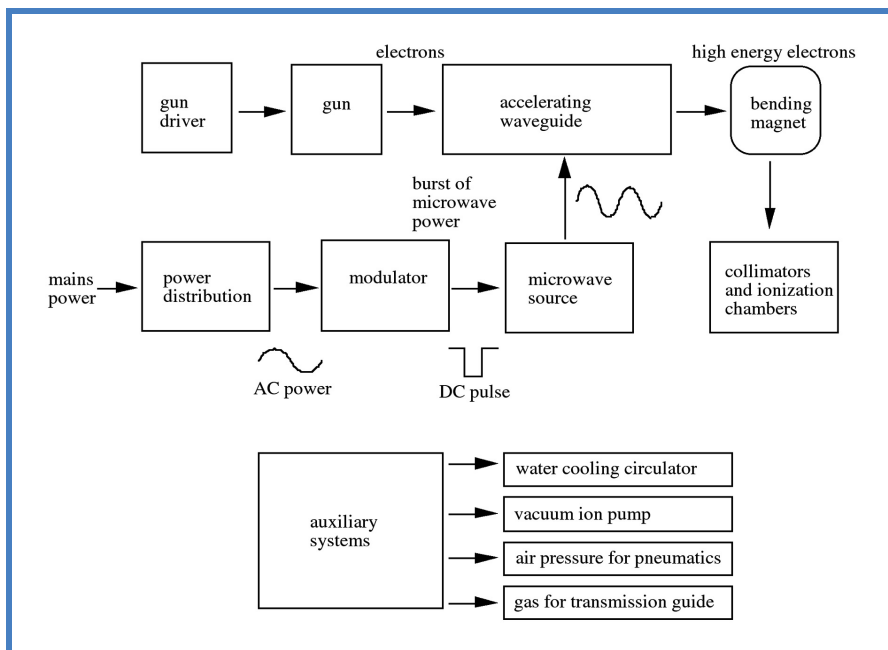


Figure 1.3 Block diagram showing linac support and auxiliary system.

gen-filled thyatron is fired, acts like a switch, discharging the voltage from the PFN. The peak current through the thyatron is about 500 amps, hence this is the only viable switching device. The resulting current passes through the primary windings of a pulse transformer. This is an autotransformer with multiple parallel windings; the low-voltage end is connected to earth, and the high-voltage end is connected to the cathode of the microwave generator. The voltage across the PFN follows a charge–hold–discharge cycle. The discharge is determined by the PFN, and the frequency is determined by the pulses applied to the thyatron to make it conduct (Greene 1986). The frequency of the thyatron switching is controlled by a *pulse repetition frequency* (PRF) generator. The microwave source is then provided with short-duration pulses from the pulse transformer.

1.3 Klystrons and Magnetrons

Linear accelerators generally employ either a klystron amplifier or a magnetron generator. These are special kinds of electron tubes that supply amplified microwave power to the accelerating waveguide structure. Microwaves are similar to radio waves (up to 450 MHz), but they have a much higher operating frequency (in the range of 3 GHz to 30 GHz). For linac operation, the microwaves that are generally used have a frequency of about 3 billion cycles per second (3000 MHz = 3 GHz). As with all electromagnetic radiation, the electric field vector, E , associated with microwaves changes sinusoidally in magnitude and direction with time. The wavelengths of microwaves are in the range of several centimeters (3 GHz equates to a wavelength of about 10 cm.) Microwave devices use resonant microwave cavities that are generally cylindrical or rectangular in cross section and several cm in diameter and length.

Figure 1.4a is a schematic of a single microwave cavity with a circular hole cut in each end to allow electrons to pass through. This cavity is used in klystron and waveguide operation. The spatial relation between the E field and the magnetic field, H , are shown in the schematic. In this case, the orientation and magnitude of the magnetic field due to the Lorentz force does not significantly affect the motion of the electrons. It is the E field that accelerates the electrons. Electrons are attracted by the E field of opposite sign at each half cycle of the microwave pulse, hence energy is transferred from the E field to the electrons at this time. This occurs in an accelerating waveguide. If the electron already has significant speed and is slowed, some energy is transferred from the electrons to the E field. This occurs in the klystron catcher cavity.

An electron traveling at high velocity in the opposite direction to an electric field can transfer much of its kinetic energy to the E field, and the energy can be expended in the form of amplified microwaves. A two-cavity klystron is shown in Figure 1.4b. The two-cavity resonators act as bunching and catching cavities connected by a drift tube. The electrons that are leading are traveling at a slower rate than those following; hence while traveling along the drift tube, the electrons are progressively bunched en route to the catcher cavity.

Electrons are accelerated from the cathode in the first buncher cavity. The buncher cavity is energized with low-power microwaves from a small microwave oscillator. This has the effect of setting up alternating E fields between the cavity walls. Note that the E field in the buncher cavity varies with time, as shown in Figure 1.4c. Electrons in position between a and b are slowed down as they encounter a

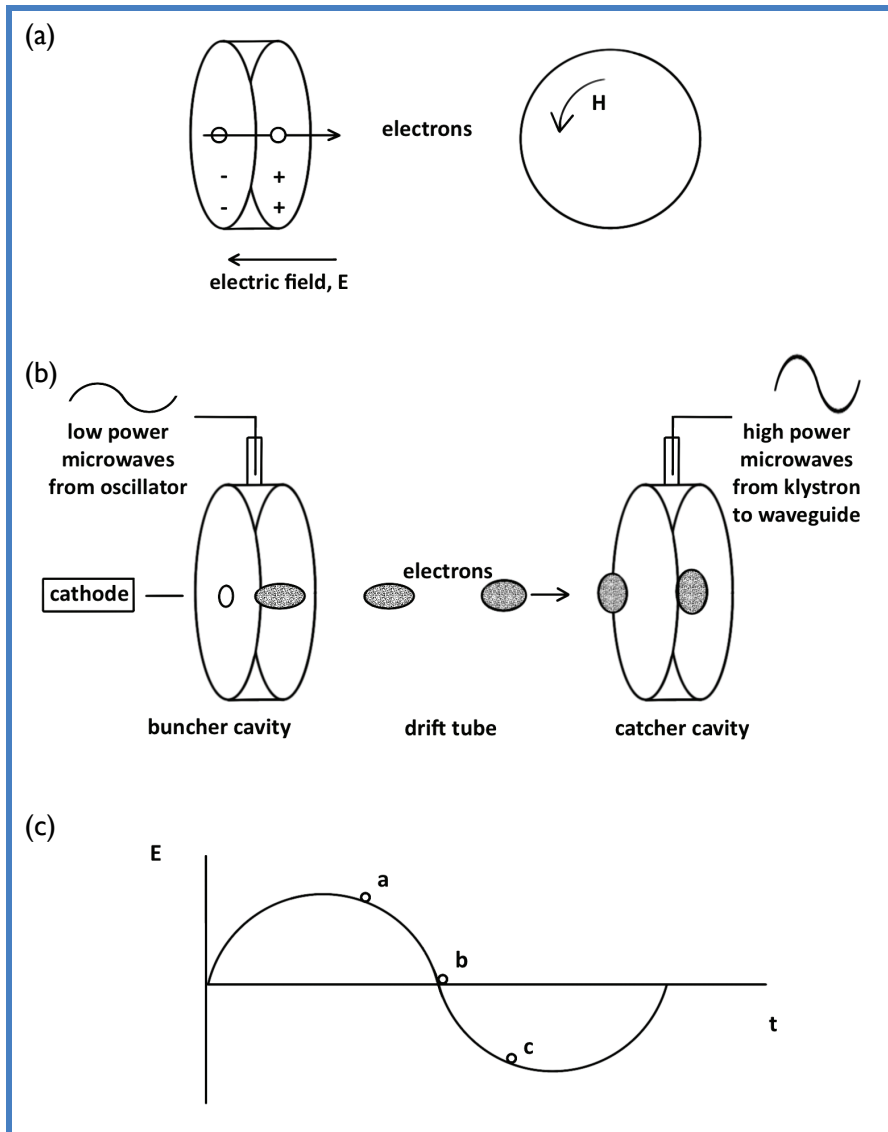


Figure 1.4

Microwave cavities and klystrons. (a) The electric and magnetic field orientations at an instant of time in a microwave cavity. (b) Schematic of a two-cavity klystron. (c) Timing diagram for the E field in the buncher cavity.

retarding E field, while those between b and c are sped up by an accelerating E field. The process is known as *velocity modulation*, and it causes bunches of electrons to form.

A catcher cavity is resonant at the arrival frequency of the bunches. As the electrons traverse the catcher cavity, they encounter a retarding E field and are slowed. During this process much of the kinetic energy lost to the electron is gained by the E field and, therefore, the microwaves.

The low-power microwaves that are fed into the input of the klystron are usually provided by a solid state oscillator at about 50 watts. This is amplified by the klystron to an output in the order of megawatts, which is used to energize the accelerating waveguide. Klystrons used in linacs usually have five cavities to improve high-current bunching and increase amplification. An amplification of microwave power in the order of 10^{11} is typically achieved by this process. Typically 7 megawatts of peak power are produced by klystrons.

An alternative way to generate microwaves of sufficient energy is with a magnetron. These are generally used to power lower-energy linacs, but this is not always the case. The magnetron is generally physically smaller and lighter than the klystron, hence klystrons are normally mounted in or behind the stand, whereas magnetrons can be mounted in the gantry. As shown in Figure 1.5, electrons emitted from the cathode are accelerated by a pulsed electric field, E_{dc} , toward the anode. The electrons produce an additional charge distribution that is shown on the anode poles and induces an electric field, E_{dc} , of microwave frequency between each segment of the anode. The electrons travel in spirals under the combined influence of the two E fields and the accompanying H field components. Most of the electron path deflection is due to the H fields. In the process, the electrons are slowed, and most of the electron beam energy is converted to microwave power. An output aerial is inserted into one of the cavities to couple the microwave power from the magnetron to the waveguide.

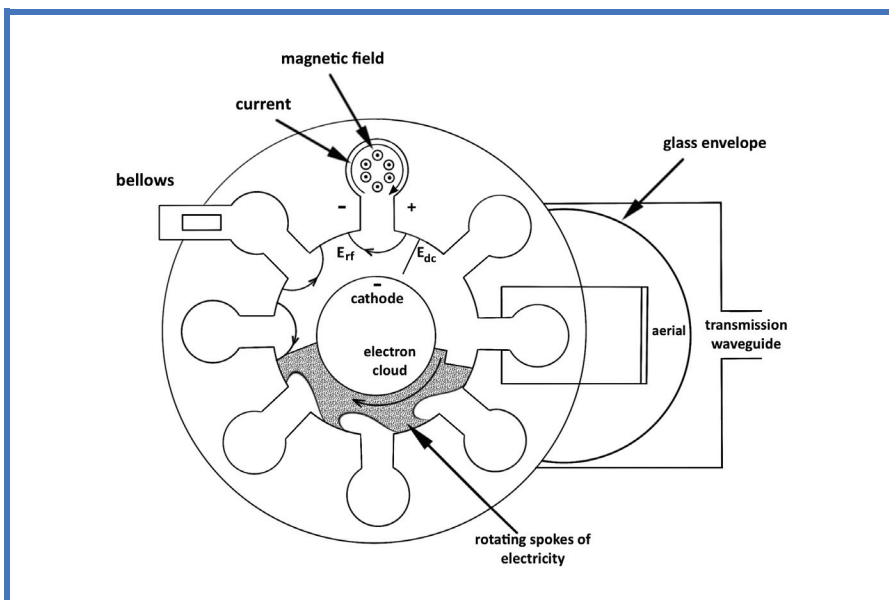


Figure 1.5

A magnetron used to generate microwaves. Electrons move in a coiled path under the influence of two electric fields: a static field E_{dc} and a pulsed electric field E_{rf} applied between anode and cathode. Because the electrons are moving in coiled paths at varying speeds, bunching occurs and microwave energy is given off. Electrons move along the negative direction of the field lines, some being accelerated and some retarded due to their phase relative to the RF field. The electrons cluster in a spoke formation that rotates around the cathode at the same velocity as the RF wave.

Magnetrons generally supply about 2 megawatts of peak power. They are referred to as *high-power oscillators* and, therefore, originators of microwave power. Klystrons require a low-power oscillator to get them started, after which feedback may be employed. This is why klystrons are generally referred to as *microwave amplifiers*.

As the magnetron is a self oscillator, it is tuned to the frequency of the accelerator structure by a small radio frequency (RF) feedback signal from the electromagnetic field in the waveguide, which activates a motorized plunger in the magnetron cavity array. The feedback mechanism is known as the *automatic frequency control* (AFC).

Microwave power is conveyed from the microwave source (klystron or magnetron) through a transmission waveguide (not an accelerating waveguide), which is filled with pressurized gas (sulfur hexafluoride, SF₆) to prevent arcing to the transmission waveguide structure. Two microwave windows—made of ceramic or beryllium, both of which are transparent to microwaves—separate the pressurized gas from the vacuum maintained in the klystron/magnetron and the vacuum maintained in the accelerating waveguide.

1.4 Electron Gun

The electron gun is the source of electrons for the accelerating waveguide. It consists of an anode and cathode and may also contain a gun grid. In its simplest form, the gun consists of a directly heated cathode in the form of a spiral tungsten filament that boils off electrons at a high temperature. The cathode is surrounded by a cone-shaped focusing electrode. Electrons are accelerated to the anode and escape through a port into the accelerator guide. The gun is usually pulsed by the same pulses that drive the microwave source.

In many modern linacs, the reliability of the gun is enhanced by using an indirectly heated cathode known as a *dispenser cathode*. These are usually made from sintered tungsten impregnated with barium oxide to enhance electron emission (see Figure 1.6). Because of the enhanced emission, this type of cathode can be operated

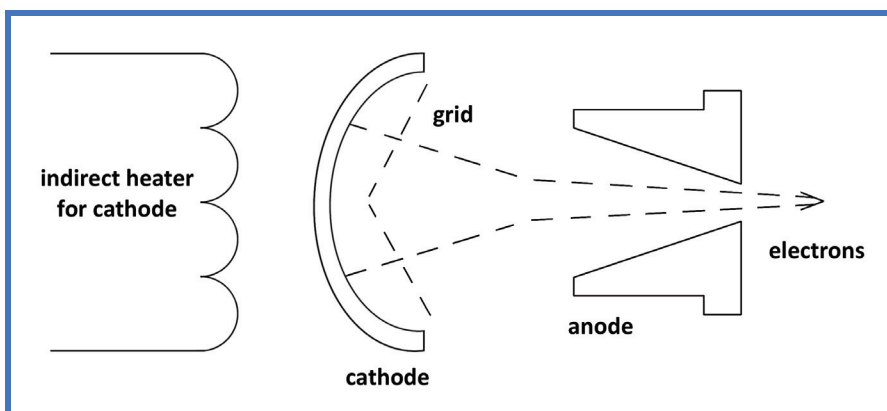


Figure 1.6 A grid dispenser type gun commonly used in modern linacs.

at a lower voltage (nominal 10 kV, versus 45 kV). During gun operation the cathode is heated to temperatures of between 1100 and 1200 degrees Celsius. Gun lifetime is important because replacing the gun usually requires the linac to be out of operation for several hours while the vacuum system is reconditioned. Some designs even require the gun and guide to be replaced at the same time.

Voltages of between -150 and $+180$ are applied to a small grid in front of the cathode to control gun current; the more positive the voltage on the grid with respect to the cathode, the higher the gun current. The gun grid controls the flow of electrons from the cathode to the anode by altering the amplitude of the grid pulses. This is usually called *gun current adjustment*. If the grid is set at -150 V there is no electron flow and, therefore, no gun current. Electrons are injected simultaneously with the high-power microwaves into the accelerating guide.

The electron gun is controlled by a gun driver subsystem. Its functions are to:

- supply a source of power to heat the gun filament,
- supply a source of high voltage for the gun cathode, and
- supply a program pulse of correct phase and wave shape for the gun grid.

1.5 Accelerator Waveguide

In the linac waveguide (which gave the linear accelerator its name), the cavity principle is applied toward an opposite goal than in the klystron, i.e., energy from the cavity's E field is used to accelerate electrons.

A hollow pipe, such as the microwave transmission guide, would allow microwaves to travel too fast for electrons to catch up. Hence, the guide is loaded by introducing cavities. Electrons are captured and bunched on the moving E field by traveling in step with the advancing E field wave.

The first few cavities increase in length, or pitch, to give the microwaves a phase velocity that matches the initial low velocity of the injected electrons. This also has the effect of bunching the electrons and is called the *bunching section* of the guide. The later cavities are of uniform pitch. Electrons quickly gain energy and reach a velocity close to the speed of light in the first few cavities. From then on, the electrons continue to gain energy according to Einstein's special theory of relativity, but they only gain a little extra velocity because most of the energy gain goes into increasing their mass.

Accelerating guides are predominantly made from copper because this material has a high electrical conductivity at microwave frequencies. This results in low power loss when microwaves are reflected off the walls of the cavities. The accelerating guide is maintained at high vacuum, typically 10^{-6} torr (1 torr = 133.3 pascal), to prevent electron loss and arcing.

To ensure that electrons are retained in focus, direction, and position within the guide, a series of buncher steering coils and focusing solenoid coils are housed around the guides.

Accelerator waveguides are of two types: the traveling waveguide type and the standing waveguide type. The principles of operation of the traveling waveguides and standing waveguides are explained as follows.

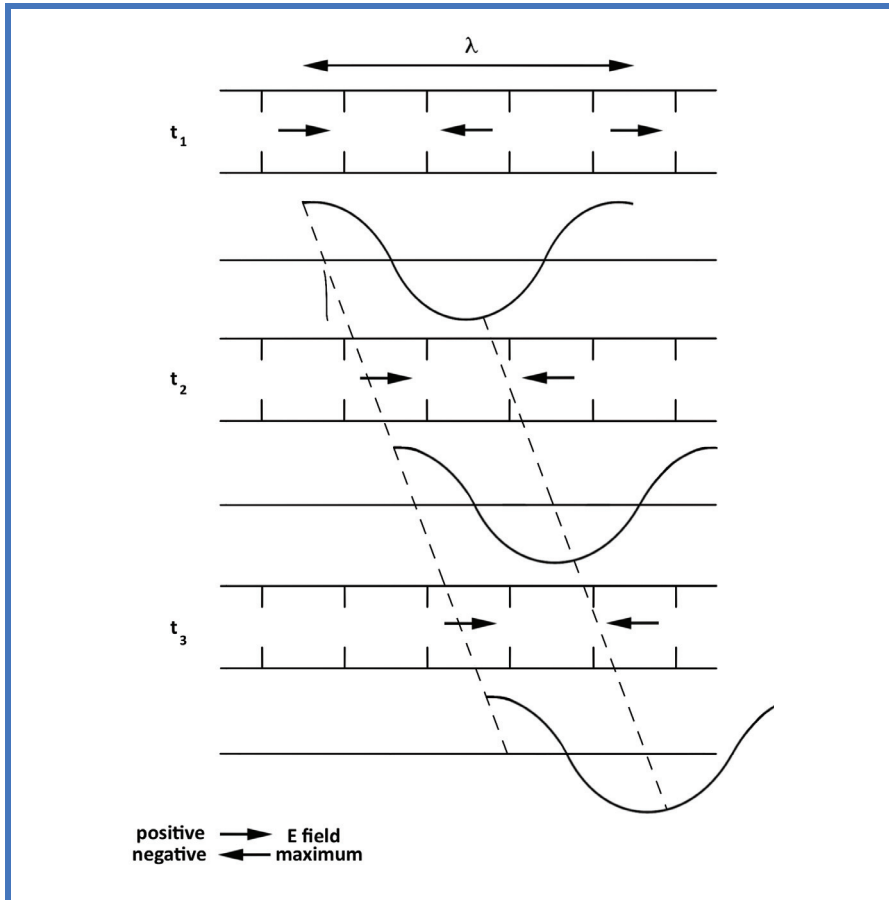


Figure 1.7 Traveling wave E field at times t_1 , t_2 , and t_3 . (Reprinted with permission from Karzmark and Morton, *A Primer on Theory and Operation of Linear Accelerators in Radiation Therapy*, 3rd Ed., Medical Physics Publishing, 2017.)

1.5.1 Traveling Waveguide Accelerator

The microwave power for a traveling waveguide is introduced at the proximal (gun) end of the guide, and any remaining microwave power at the other end of the guide is absorbed by a microwave power load; none of the power is reflected.

Electrons injected by the electron gun are captured and bunched on the traveling E field, and they gain energy by traveling in phase with the advancing E field. Figure 1.7 shows a typical traveling wave E field moving to the right in the accelerating waveguide at three sequential instants of time t_1 , t_2 , and t_3 . These time sequences are separated by one quarter cycle of the microwave pulse in time. Figure 1.8 shows the spatial relation of the traveling wave E field at one instant in time. The electron bunches as shown are pushed by the negative charges and pulled by the positive charges along the wave guide.

There are four cavities per microwave wavelength. Each cavity is several centimeters long, which requires a rather long guide. In general, traveling waveguides are longer than standing waveguides when generating electrons of the same energy.

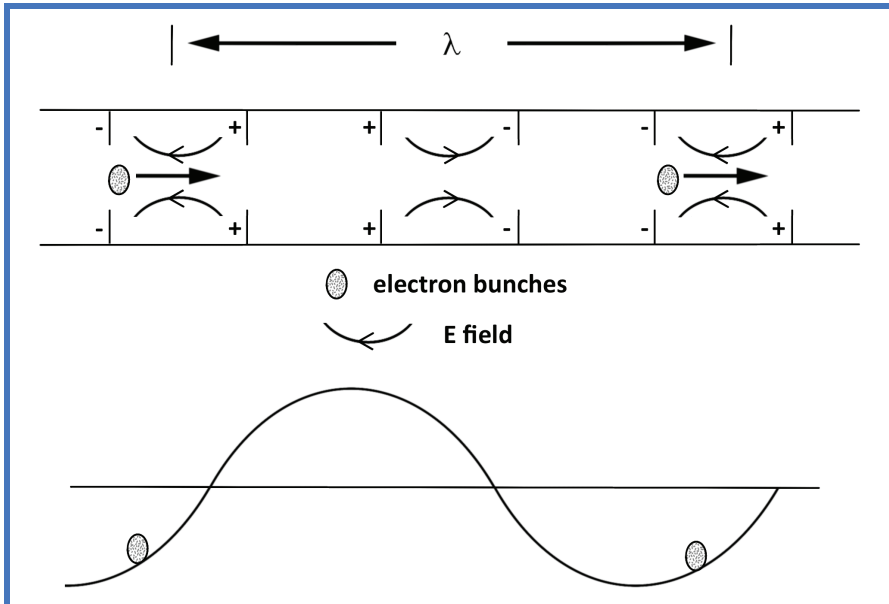


Figure 1.8

Charge distribution in a traveling wave accelerator in which electrons are accelerated. (Reprinted with permission from Karzmark and Morton, *A Primer on Theory and Operation of Linear Accelerators in Radiation Therapy*, 3rd Ed., Medical Physics Publishing, 2017.)

I.5.2 Standing Waveguide Accelerator

In contrast to traveling waveguide accelerators, the microwave power in the standing waveguide accelerator is not absorbed at the end of the waveguide, but is instead reflected back down the guide. This gives rise to standing waves that do not travel down the guide, but oscillate in magnitude with time. Standing waveguides require a device that deals with unwanted reflected power in the guide. Microwave power is fed into the guide (at any location along its length) via a device called a *circulator* (usually having three or four ports). The circulator is a directional coupler designed to introduce the power at resonant frequency and also to act as a channel for the rejected energy via one of its ports to a water load.

Shown in Figure 1.9 is the E field distribution for a standing wave accelerator. The upper arrow in each cavity represents the direction of the E field in the incident wave, and the lower arrow represents the direction of the E field from the reflected wave. The effective E field in each cavity is the sum of the incident and reflected E fields. Note that every second cavity has a forward and a backward E field component which, when summed, gives a resultant zero E field in the intervening cavity. However, these cavities that contain no E field are essential to couple power between the accelerating cavities.

To reduce the length of the accelerating waveguide, these cavities can be moved to the side of the accelerating structure, away from the accelerating electron axis, as shown in Figure 1.10. Most linac waveguides employ this array of side-coupled cavities in their standing waveguide design. Using this design, a stronger electric field is obtained than with a traveling waveguide, and a shorter guide can be used to achieve the same electron energy.

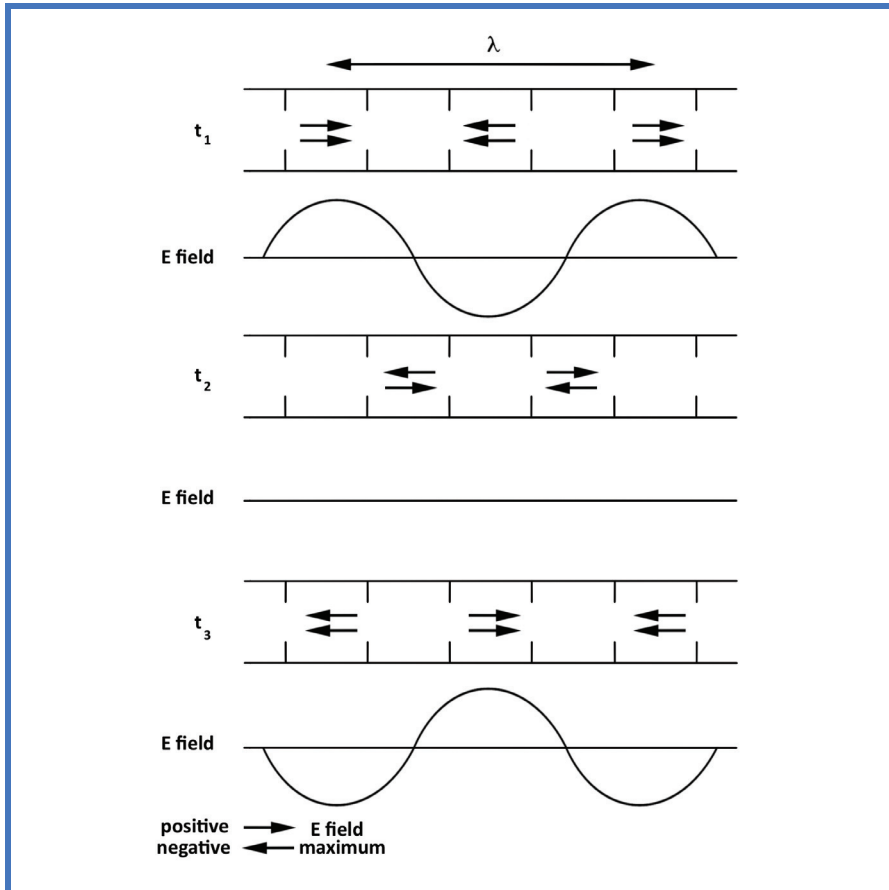


Figure 1.9

Standing waveguide E field distribution at times t_1 , t_2 , and t_3 . (Reprinted with permission from Karzmark and Morton, *A Primer on Theory and Operation of Linear Accelerators in Radiation Therapy*, 3rd Ed., Medical Physics Publishing, 2017.)

Figure 1.11 shows a sequential look at the E field from times t_1 to t_9 over a complete microwave cycle for a standing wave accelerator. Injected electrons from the gun are captured, bunched, and accelerated in the first few cavities. They then pass through the next cavities in a negative E field and are accelerated. At this time the next cavity has a positive E field and no electrons can be accelerated in it, which doesn't matter because at this time the electrons have not reached this cavity. As the electrons cross into the next cavity, the E field in this cavity starts its negative excursion, and the electrons are further accelerated.

The microwave frequency is about 3 GHz. The magnetron or klystron receives 5-microsecond pulses from the PFN with a 5-millisecond gap between pulses. Note that there are actually thousands of pulses in each sequence. It has been estimated that there are 10,000 electrons carried in each 30-picosecond microwave pulse, and each pulse has an approximate 300-picosecond separation with about 150,000 electrons in each 5-microsecond packet of pulses (Krieger and Petzold 1989). Shown in Figure 1.12 is a typical pulse sequence, including the pulse-forming network pulse, which is visible using an oscilloscope.

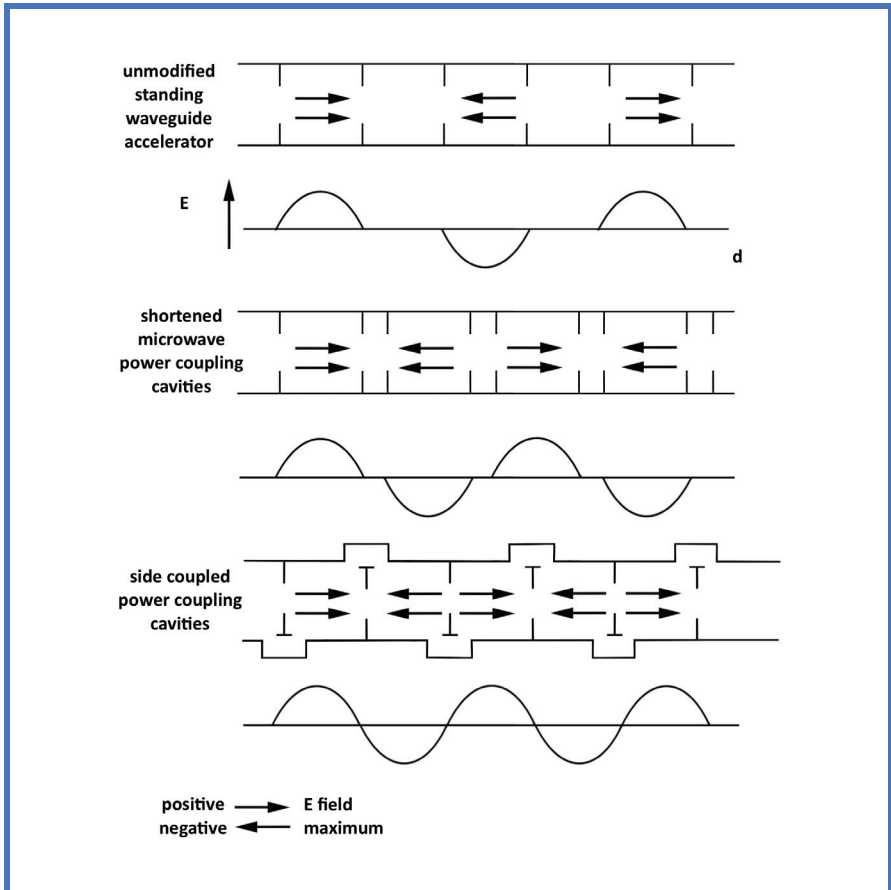


Figure 1.10

The evolution of the side-coupled standing waveguide design. (Reprinted with permission from Karzmark and Morton, *A Primer on Theory and Operation of Linear Accelerators in Radiation Therapy*, 3rd Ed., Medical Physics Publishing, 2017.)

Example 1.1

Question: A linac is delivering a dose rate of 2 Gy/minute to a calibration point within a water medium. The radiation is in 5-microsecond pulses (assuming the pulses are continuous), and the pulse period is 5 milliseconds. Calculate the instantaneous dose rate during a pulse.

Answer: The dose rate is 2 Gy/minute, which is $2/60$ Gy/second. The pulses have a 5-millisecond period, which means there are 200 pulses per second.

The dose per pulse is $\frac{2}{60 \times 200} = 1.67 \times 10^{-4}$ Gy. Therefore, the dose rate in the pulse per minute equals the above value multiplied by 60 to get to dose per minute and divided by 5×10^{-6} , as this is the pulse period. This gives an instantaneous dose rate within the pulse of 2000 Gy/minute.

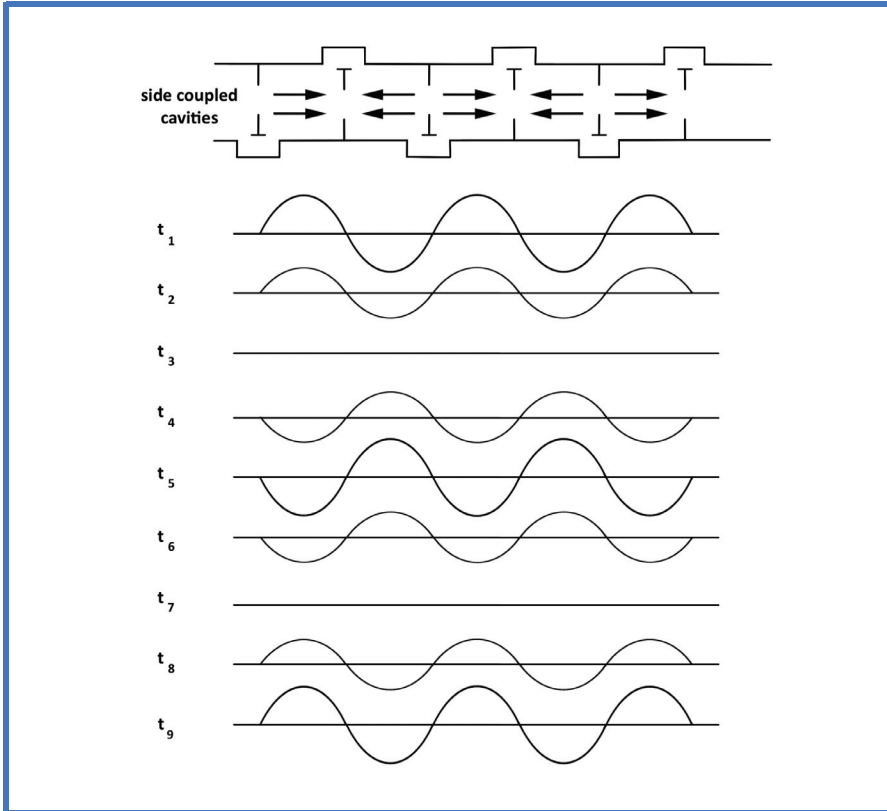


Figure 1.11 Standing wave E field pattern for one full microwave cycle shown at nine discrete time intervals. (Reprinted with permission from Karzmark and Morton, *A Primer on Theory and Operation of Linear Accelerators in Radiation Therapy*, 3rd Ed., Medical Physics Publishing, 2017.)

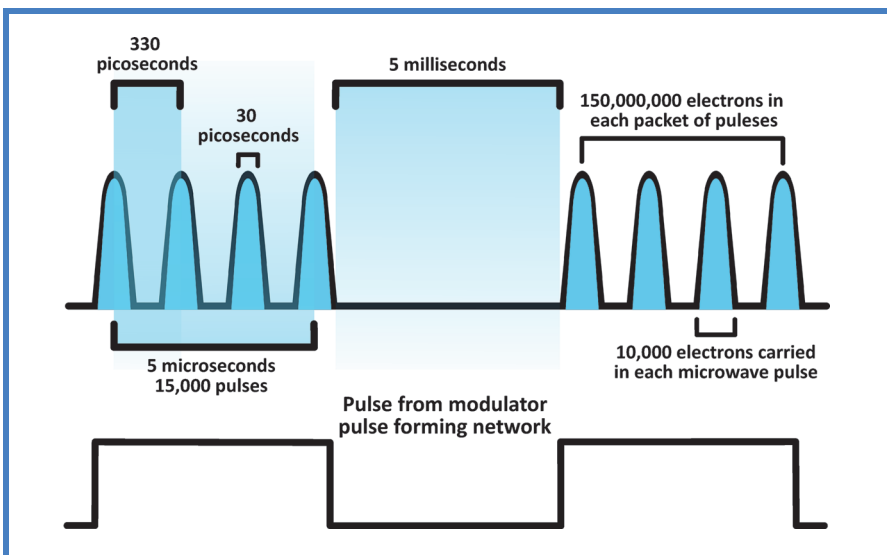


Figure 1.12 Linac x-ray and electron beam pulsed beam delivery. Figure shows typical times from the pulse-forming network and the approximate number of electrons in each wave packet. (Courtesy of Saree Alnaghy, University of Wollongong.)

Table 1.1 Features of traveling and standing wave accelerator structures used for linacs

Parameter	Traveling Wave	Standing Wave
electron acceptance	high	low
electric field strength	low	high
length of guide	longer	shorter
microwave power feed	at gun end	anywhere
acceleration	continuous	pulsed
frequency dependence	low	high
phase dependence	low	high
guide loading	low	high
vacuum requirements	lower	higher

1.5.3 Energy Selection

In electron mode, the linac can be tuned for different electron energies by adjusting the microwave power in the waveguide and the electron current. Increasing the beam current progressively extracts an increasing fraction of the RF power from the guide; this is known as *beam loading*. When the gun current levels are low for electron beams, the amount of RF power being extracted is small, which means the load line is reasonably flat. Tuning for different electron energies using this method is effective.

However, for x-ray production to ensure sufficient bremsstrahlung production through the target, the gun current is much higher. This is typically 600 mA for 6-MV x-rays versus 150 mA for 18-MeV electrons. At these levels of gun current, the load line is very steep, and retuning for different energies is more challenging for standing waveguide machines. A number of methods for creating different energies are discussed elsewhere (Karzmark and Morton 2017). One practical method for producing low- and high-energy x-rays in a standing waveguide that does not compromise dose rate is the use of an energy switch. The switch drives into part of the accelerator structure, decoupling the second part of the waveguide so that only the first part is used. The electrons then reach the end of the guide without further acceleration. The whole length of the guide can be used to produce high-energy x-rays. In traveling waveguides, the second portion of the RF field can be tapered down to produce low-energy x-rays (Karzmark and Morton 2017). Table 1.1 is a summary of the different properties of traveling and standing waveguide designs.

1.5.4 Electron Energy

When electrons are accelerated to relativistic velocities, the mass, m , and energy, E , are related, as postulated by Einstein's theory of relativity (1905), such that

$$E = mc^2 \quad (1.1)$$

where c is the speed of light.

Hence, the kinetic energy, E_k , given to an electron accelerated in a linear accelerator waveguide is

$$E_k = mc^2 - m_0c^2 \quad (1.2)$$

where m_0 is the electron rest mass (9.11×10^{-31} kg). By rearranging Equation (1.2) then

$$m = m_0 + \frac{E_k}{c^2}. \quad (1.3)$$

The particle's mass, m , is related to m_0 by

$$m = \frac{m_0}{\left(1 - \frac{v^2}{c^2}\right)^{\frac{1}{2}}}, \quad (1.4)$$

where v is the velocity of the particle. By rearranging Equation (1.4) then

$$v = c \left(1 - \frac{m_0^2}{m^2}\right)^{\frac{1}{2}}. \quad (1.5)$$

Example 1.2

To acquire a feeling for the quantities involved when dealing with linear accelerators, let us apply the above equations to a typical electron energy. By applying equation 1.3 to a 6-MeV electron beam ($1 \text{ MeV} = 1.602 \times 10^{13}$ joules), the result is that the electron acquires a mass $m = 12.7 m_0$. By applying Equation (1.5), the velocity of the electron $v = 0.994 c$, which is within 0.006 of the velocity of light.

1.6 Beam Delivery

1.6.1 Bending Magnet Assembly

For low-energy standing wave linacs (generally up to about 6 MV) the waveguide is short enough (about 0.4 meters) to be mounted vertically in the gantry while still enabling full 360-degree gantry rotation with only a small floor inset to ensure a low couch position at isocenter. For these short waveguide linacs, electrons are accelerated toward the patient at isocenter with no further major beam steering required.

However, for virtually all traveling wave accelerators—and for higher-energy standing wave accelerators (those that produce x-ray energies greater than 6 MV)—the guide is longer (e.g., an 18-MV standing waveguide is 1.5 meters long). These waveguides have to be mounted horizontally within the gantry. In this orientation, the accelerated electrons at the end of the guide have to be bent toward the patient.

In theory, only a 90-degree bend is required. Some linacs employ the 90-degree design as it produces a more compact bending magnet and, hence, a more compact head with greater patient separation.

In practice, however, many linacs use a 270-degree bending magnet, as shown in Figure 1.13a and 1.13b. This is because the electrons get a long exposure to the magnetic field, during which time electron spectral spread or directional spread can be refocused by the bending magnet. The magnet is said to be *achromatic* because different energy electrons are drawn through a different path length and refocused

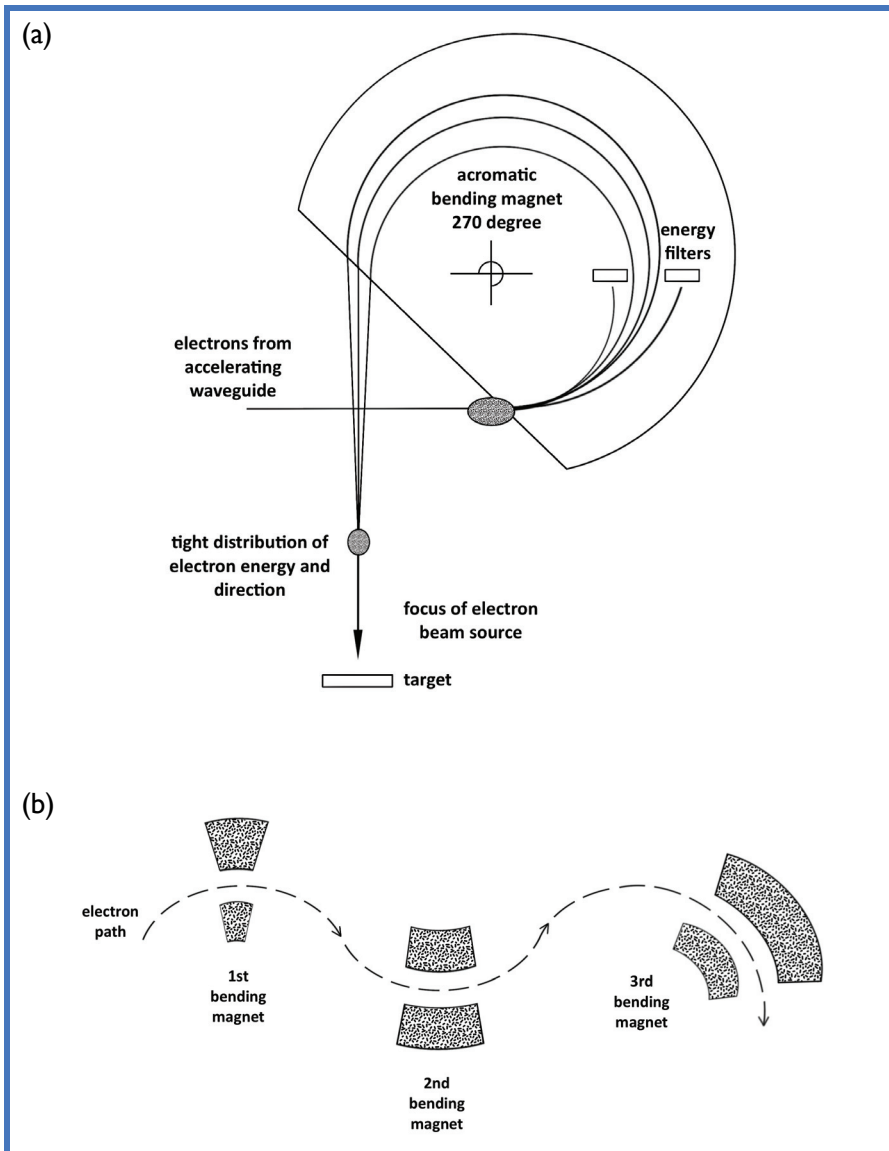


Figure 1.13

(a) Linac bending magnet design for a 270-degree bending magnet and achromatic energy slits. (b) Slalom design used to create 90-degree bend at end to enable efficient head-to-patient separation.

at the desired position. This focus of electrons is needed to maintain a small virtual beam source size. Most of these magnet designs are fitted with an energy slit that removes electrons that are not within 5% of the nominal peak accelerated electron energy. The radius of curvature of less or more energetic electrons is different; therefore, the energy slit acts as a physical barrier and removes electrons from the beam path. In practice, three 90-degree magnets are usually used, connected by short drift tubes. This, in effect, reduces the height of the machine isocenter because the target can be mounted closer to where the electrons enter the magnet.

Some accelerators use magnets to deflect electrons by small angles within the guide, with the final deflection being about 90 degrees (see Figure 1.12c). This is known as a *slalom waveguide* as employed by some Elekta linacs, and this has some perceived advantages:

1. It reduces the length of the guide.
2. It acts as an achromatic device, tightening the energy spectrum of the electrons.
3. It lowers the machine isocenter height.

1.6.2 Target and Flattening Filter

The narrow electron beam is converted to a broad x-ray beam by bremsstrahlung production in a target (usually made of copper). The target may be a pneumatically driven device. Different thicknesses of copper are used. Lower-energy photons require less thickness of copper, as shown in Figure 1.14a, where the deeper recess is for the lower-energy x-ray target and the shallow recess is for the higher-energy target. The high-energy x-rays emerging from the target are forward peaked in a bullet-shaped lobe that is further collimated by a fixed primary collimator.

To create a uniform beam, the x-ray dose profile is flattened by a flattening filter that is shaped like a cone with the point of the cone facing the target. This is made of tungsten, steel, or a lead/steel combination. Two flattening filters are shown in Figure 1.14b.

The cross-beam profiles of large fields generally have a slightly higher dose near the edges than in the central axis; these high-dose regions are referred to as *dose horns*. Dose horns arise because the flattening filter is a compromise design to ensure a nearly flat beam profile at all field sizes. The horns contain low-energy components that may be attenuated more rapidly through the medium. This is because the beam flattening filter is narrower at the edges than in the beam's central axis. The horn effect tends to dissipate with depth, and by about 10 cm depth the horns are generally less than they are near the incident surface.

If electrons, instead of x-rays, are to be used to treat the patient, the target and flattening filters are generally replaced by an electron scattering foil. During a change of mode from x-rays to electrons, the target is retracted, the flattening filter is driven out of the beam, and the foil is placed in the beam path. The beam gun current is also significantly reduced. All of these operations are monitored and interlocked to ensure that the correct programming is achieved. The x-ray flattening filter and electron foils are usually mounted below the target on a circular mechanism, which is referred to as the *carousel*.

The target is usually pneumatically driven into position, and there are several interlocks to ensure the machine can only operate in the selected mode. The target, foils, and flattening filter all have fault-detecting interlocks and backups to ensure correct operation. Linacs with vertical guides generally have a fixed target/flattening filter, which reduces the space and, hence, the height of the machine, but precludes the use of electrons.

1.6.3 Monitor Unit Ionization Chambers

A photograph of a monitor unit ionization chamber used in a linac treatment head is shown in Figure 1.14c. After the flattening filter, the beam traverses two parallel plate multichannel ionization chambers, as shown schematically in Figure 1.15. These are referred to as *monitor unit ionization chambers* because the monitor units are accrued using these chambers. The ionization chambers are usually made of

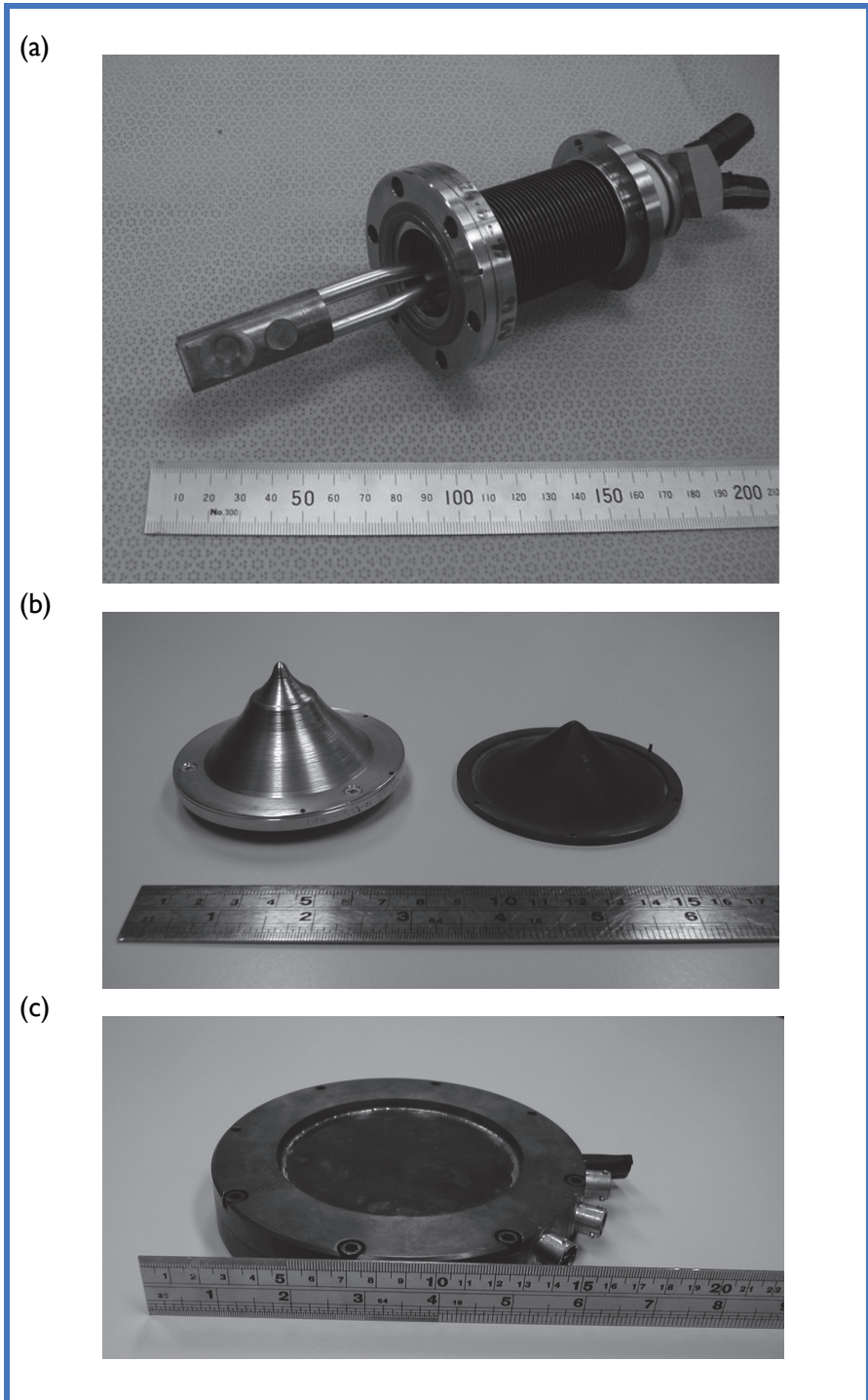


Figure 1.14 Components within a Varian linear accelerator treatment head. (a) Target from a linear accelerator with two different thicknesses of material for bremsstrahlung production for 6 MV (left) and 10 MV (right). The target is water cooled. This target resides inside the guide vacuum, hence the seals and bellows. It is pneumatically driven into one of three positions: out (electrons), 6 MV, and 10 MV. (b) Two flattening filters from a linear accelerator: 18 MV (left) and 6 MV (right). (c) External view of a monitor unit ionization chamber assembly from a linac.

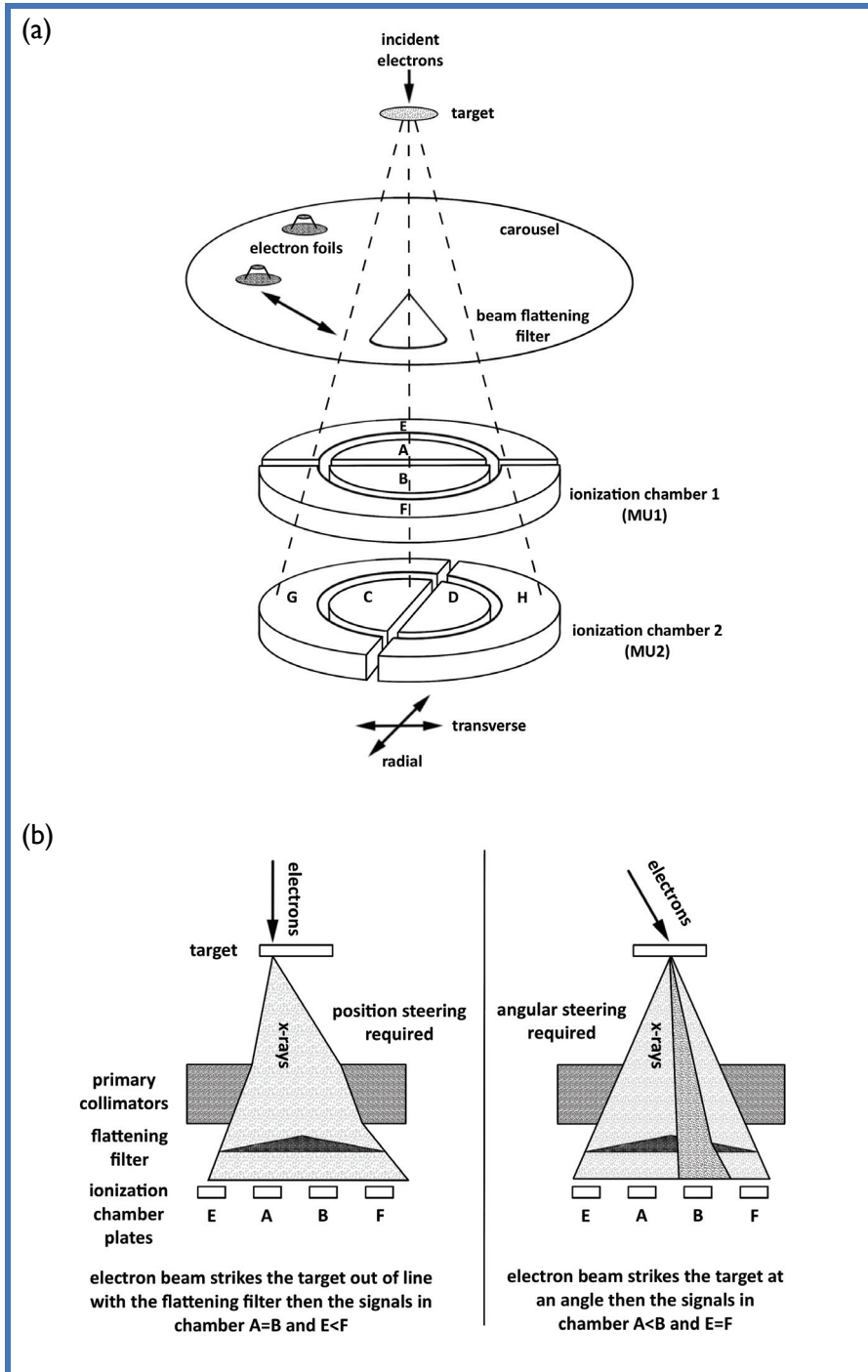


Figure 1.15 Schematics of a monitor unit ionization chamber assembly. Orientation of the ionization chambers mounted in the treatment head used to monitor dose output, symmetry, and flatness is shown. AB and CD ionization chambers are used for integration of charge to give dose output in monitor units. (b) The A to B and C to D current ratios are compared for feedback to angular beam steering in the radial and transverse planes. The E to F and G to H current ratios are compared. The current signal from the monitor ionization chambers to the electronic beam steering control circuit in the bending magnet is used to tune the beam for symmetry.

Kapton[®]. Mica was previously used, but because of a shortage of this material, Kapton is now more common. The bremsstrahlung contamination from Kapton chambers in electron mode is also less.

The mica chambers were usually filled with nitrogen, whereas the Kapton chambers are filled with oxygen-enriched air. Both of these types of chambers are sealed to avoid the necessity of correcting for changes in gas density within the volume due to ambient pressure and temperature variations. Some linacs use chambers that are not sealed; these generally have an accurate electronic temperature pressure compensation device.

The monitor unit ionization chamber plates are mounted so that one is at a 90-degree rotation offset from the other. This enables them to also monitor beam symmetry and flatness in the beam's radial and transverse planes, respectively. Beam flatness and symmetry are controlled by feedback circuits that run from the ion chambers to the bending magnet's beam steering coils. Figure 1.13e shows how the dose to the chamber plates will alter due to positional and angular deviations in beam steering. The prescribed dose needs to be delivered reproducibly for each patient treatment. To achieve this routinely, one set of the monitor ionization chambers' plates (the inner plates) are used to monitor dose output. The units of dose recorded by these are referred to as *monitor units* (MU); one MU of dose has been delivered when the monitor chambers have detected a preset dose. Because these chambers are located above the final beam collimation system, an MU setting is calibrated to a standard dose for a standard field setting. For example, 1 MU may be calibrated to equal 1 cGy at 100 cm source surface distance (SSD) for a 10×10 cm² field size at d_{\max} in water. However, 1 MU will equate to a different dose at a different field size as the collimator and phantom scatter changes depending on the field size.

The monitor chambers are interlocked to stop beam production at an operator preset dose level. As mentioned for the symmetry monitoring, there are two sets of monitor ionization chambers. They are linked to two independent calibration circuits. One is a backup to ensure that if the primary channel fails, the other channel will terminate dose. The backup is set to terminate dose at a small margin beyond the primary interlock.

Further dose regulation, apart from the monitor ionization chambers, includes a timer that terminates dose at a preset time. This means the treatment will terminate due to the time interlock if both ion chambers fail. Care is taken to ensure that the time is set slightly longer than the time needed to deliver the dose, provided the preset dose rate is achieved. If a significantly lower-than-expected dose rate is being given, the treatment may also be terminated first by the time interlock.

Of course, the operator can terminate treatment at any time by using the beam-off button on the control console. This termination usually occurs if patient movement is detected within the room via the in-room video monitors. If this occurs, the treatment is suspended, and the patient is realigned into the correct position prior to completing delivery of the prescribed dose. A two-way audio monitor is also provided for patient-operator communication.

1.6.4 Electron Beam Delivery

Modern linacs are also capable of producing clinically useful electron beams. In this case, the electron beam is not directed onto a target but used directly. Therefore, the production efficiency of electrons is much higher than for photons and, in

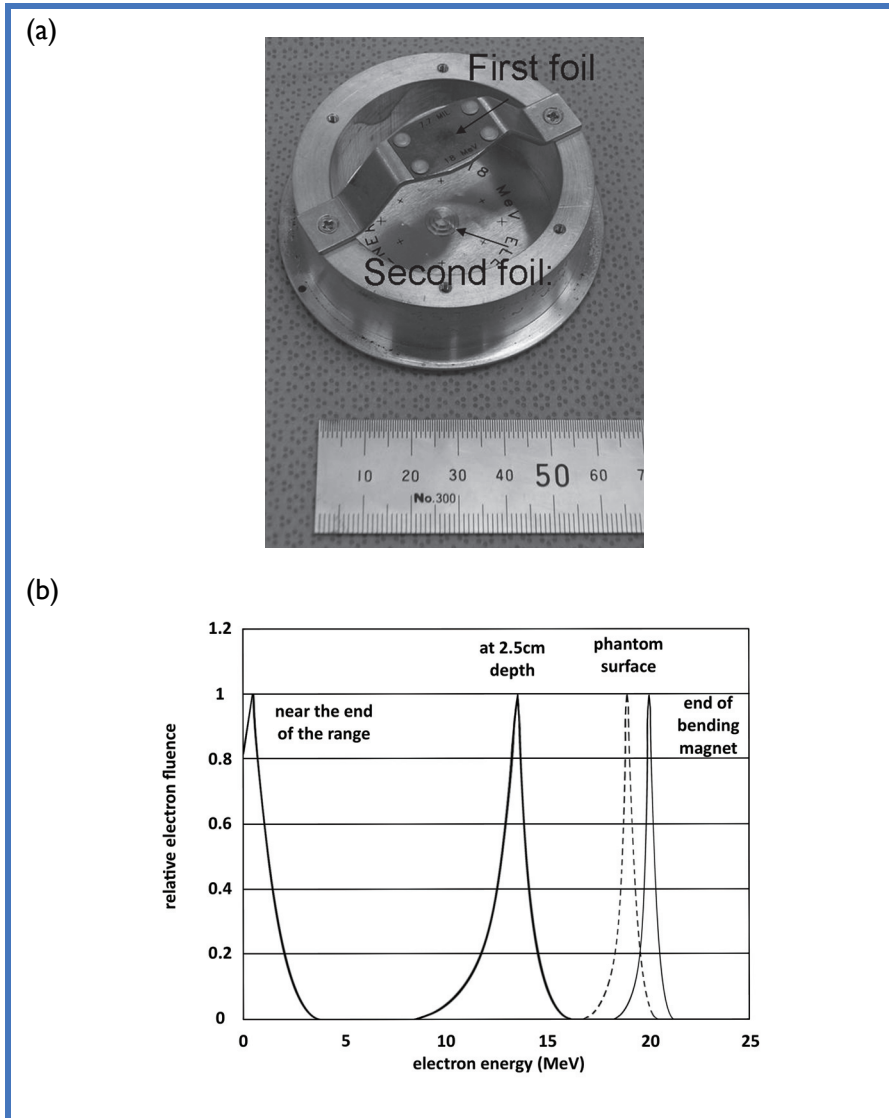


Figure 1.16 Electron scattering foils and spectrum. (a) Two-stage 18-MeV electron scattering foil from a Varian linac. (b) Typical spectral energy spread for an electron beam showing how the energy changes as the electrons move from the scattering foil to the patient surface. The spectral energy at 2.5 cm depth and the depth near the end of the electron practical range is also shown. This indicates the rapid decrease in electron energy with depth.

principle, the dose rate for an electron beam could be much higher for electrons than for x-rays.

For safety and dosimetric reasons, the electron gun current is typically reduced, and the power of the magnetron or klystron may also be reduced so electrons are delivered at similar dose rates to x-rays when used in that mode.

Most linacs producing electron beams employ a bending magnet to ensure a relatively monoenergetic beam. The energy selection slit is typically set to allow

electrons with a window of some 3% around the nominal energy through the bending magnet. Modern linacs typically have five or more electron energies available.

After the bending magnet, the electron beam has a diameter of only a few millimeters. In order to create a useful clinical beam, the electron beam must be spread out. Two methods have been used in different linacs:

1. ***A magnetic field can be used to scan the electron beam across the area to be irradiated.*** This is similar to a television screen and has been used historically in some linac systems. This technique produces a superior beam in terms of energy definition, i.e., the beam spectrum has a very small spread. Photon contamination is also reduced as none is introduced by the absent scattering foil. However, the beam steering requires additional quality assurance, and there is a high instantaneous dose rate in the scanned beam, resulting in dosimetric difficulties. Therefore, in the interest of safety, most commercially available linacs employ a scattering foil.
2. ***A scattering foil is employed in most current linac designs.*** Most linacs use a dual scattering foil as shown in Figure 1.16a. The foil device shown is for a Varian 18-MeV electron beam. Note the device houses two foils, and there are different foils mounted at different locations on the carousel, each optimized for different electron energies. The design constitutes a compromise between producing a large enough useful beam and limiting both energy degradation and bremsstrahlung production.

Because the electrons have not interacted with a target, the beam spectrum is closer to a monoenergetic beam of the peak energy, as shown in Figure 1.16b. Electrons as charged particles do interact more with air than photons, and this leads to some energy degradation as the electrons traverse away from the scattering foil. There is also an increase in angular scattering. In order to achieve a relatively well-defined beam edge, it is necessary to collimate the beam as closely as possible to the patient. This is achieved using an electron applicator, as shown in Figure 1.17a. The applicator has several planes in which the beam is collimated. The final collimation plane allows placement of an insert made from a *low-melting alloy* (LMA) in the applicator. This insert allows customization of the final collimation to individual patients. Figure 1.17b illustrates schematically the role the applicator and other collimators play in the setup used on a linear accelerator to generate and transfer a useful clinical electron beam to a patient.

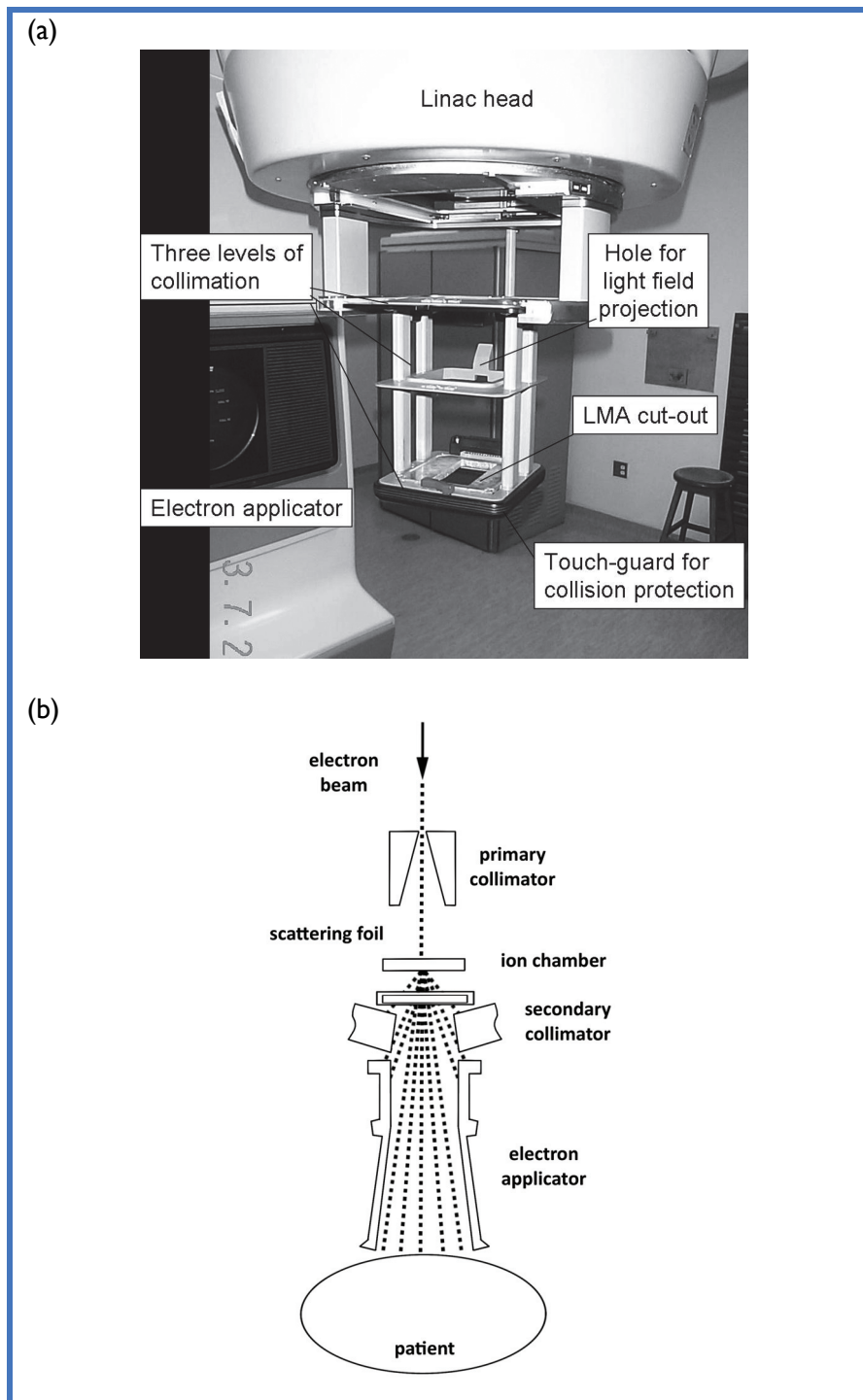


Figure 1.17 (a) Electron applicator used to improve scattering properties when electrons are employed. This applicator is placed on the block tray holder during electron mode and, when used at 100 cm SSD, the applicator is offset 5 cm from patient skin. An insert is mounted in the applicator to create an irregular-shaped electron field. (b) Schematic showing the electron applicator design in relation to the linac head components and how the device restricts scattered electrons from escaping.

1.7 Collimation

Various devices are used to collimate and modify the intensity of the x-ray beam. These devices are reviewed in the following sections.

1.7.1 Primary Fixed Collimator

A primary fixed collimator (generally made from tungsten) is mounted below the target and above the flattening filter. Shaped like a slightly diverging cone open at both ends, this device allows only forward-scattered x-rays to escape the linac (see Figure 1.3). This collimator helps prevent head leakage, e.g., scattered photons escaping from the treatment head. The dimensions of this collimator are generally such that a circular beam of approximately 50 cm in diameter would be incident at 100 cm SSD if the secondary collimators were not present.

1.7.2 Secondary Collimators (Jaws)

A secondary collimation system consists of two pairs of metal blocks usually made from tungsten or lead alloy about 8 cm thick. The common names given to these devices are *collimators* or *jaws*. The transmission through the jaws is about 0.4% of dose due to the unshielded incident beam. The collimators can be adjusted to produce different rectangular field definitions from 0 cm to 40 cm for each jaw incident at the patient. The collimators are also able to rotate around the beam's central axis; this is referred to as *collimator rotation*.

As the jaws are extended, they tilt so that the jaw face angle equals the beam edge divergence angle. As both sets of jaws match beam edge divergence, this is known as a *double focused collimator*. This ensures that the full jaw face is parallel to the edge of the x-ray beam. If the jaws were not so aligned, this would lead to a broader beam penumbra due to partial jaw transmission. A combination of couch, collimator, and gantry angle can provide beam incidence at virtually any required treatment angle.

When used in electron mode, the secondary collimators are usually opened wider than the required field, and final collimation is provided by an electron applicator. This is a demountable device that attaches to an accessory mount and provides collimation at about 5 cm from the patient surface. This is required because electron scattering in air produces a wide beam penumbra if the collimators are farther away, and a bremsstrahlung edge is created if placed directly on the skin.

A *visible light field* defines the geometric center and edges of the radiation field. On most modern linacs the light field is produced by a projector-type light source reflected from a thin nonretracting mylar mirror set in the head of the machine just above the collimators. Variations in design include retracting mirrors and lights placed on a slide in the target mount. The center of the field is sometimes defined by a crosshair etched onto a thin Mylar window mounted below the jaws, and the edge of the light field is defined by the jaws. The optics should be calibrated so that light field divergence and radiation field divergence agree over a range of clinically used SSDs.

1.7.3 Asymmetric Collimators

Linacs have independent drives for each collimator to enable definition of asymmetric fields. For example, as Figure 1.18 shows, instead of having a field with symmetry in both axes, one of the jaws can be driven closer to the center of the field

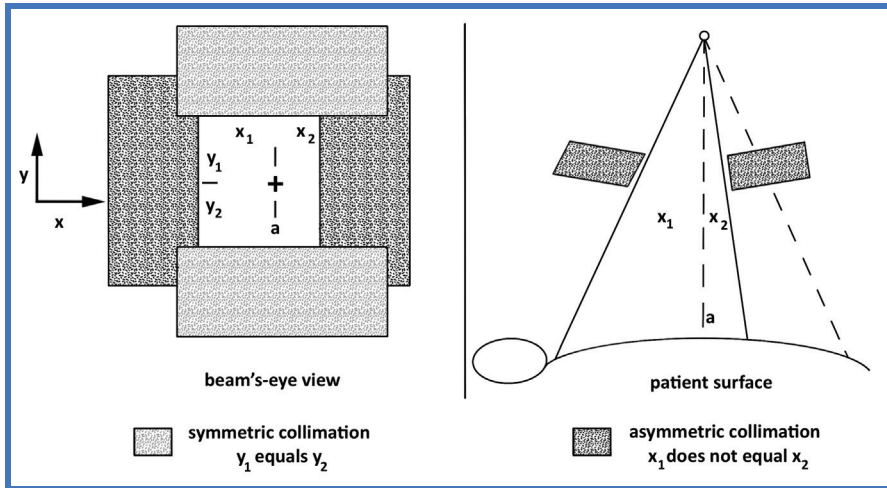


Figure 1.18 Asymmetric collimators from a beam's-eye view and side view perspective. Both sets of collimators can be set asymmetrically or symmetrically about their axis.

and the other jaw driven farther from the central axis. This creates an asymmetric field with the x_2 jaw closest to the central axis providing a less-diverging edge, while the other jaw, x_1 , has a more diverging field edge.

1.7.4 Blocks

The two sets of collimators can only provide rectangular field shapes on the patient surface. Therefore, other devices were historically used to create irregular field shapes so that organ-at-risk structures—such as heart, lung, or spine—may be shielded from the x-rays.

Lead blocks (see Figure 1.19) were historically used to modify the x-ray treatment field dose distribution. These were mounted on trays known as *block trays* that slide into a removable accessory tray mounted at the end of the treatment head. Block trays were usually made from acrylic or polycarbonate that was transparent, so in combination with the light field this was suitable for field alignment with patient skin tattoos. (Typical dimensions were 30 cm × 30 cm × 0.6 cm.) Block trays created extra electron contamination in the beam, thus increasing patient skin dose. They also attenuated the beam (typically by about 3%), and a block tray correction factor for beam output was applied.

Block thickness was generally sufficient to provide at least five *half-value layers* (HVLs) of shielding. Each linac used to have a set of lead blocks in standard shapes, in particular a set of long, narrow blocks for spinal cord shielding. Low-melting-point alloy (LMA) was also used in some radiotherapy departments to shape blocks for irregular x-ray fields. The molding of LMA into irregular shapes is still common for creating electron inserts for electron treatments. The density of lead is 8.3 g cm⁻³ versus 11.3 g cm⁻³ for LMA. Blocks now play a very limited role in radiotherapy. The introduction of multileaf collimators have rendered blocks virtually redundant.

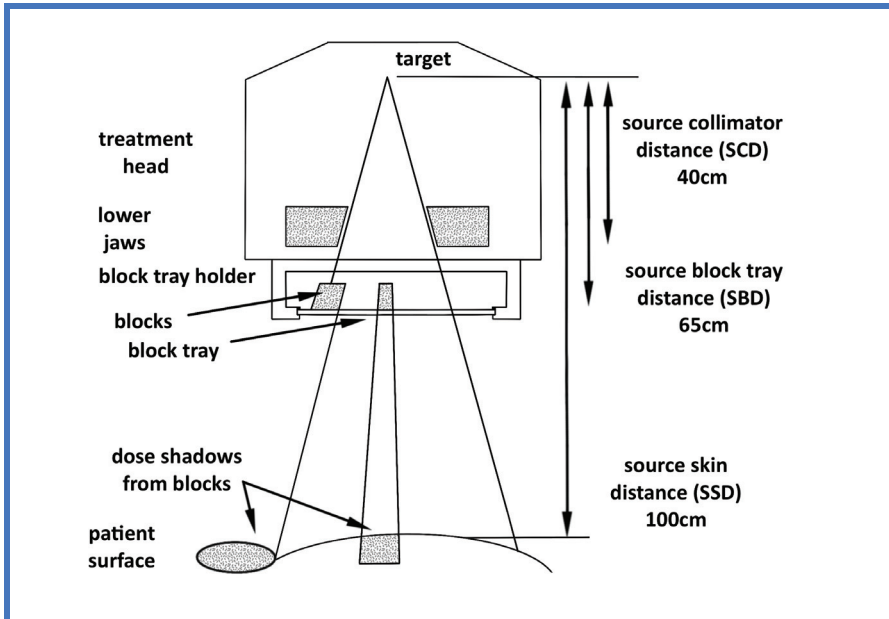


Figure 1.19

Blocks that may be placed on the accessory tray mount on a block tray at the exit position of the linac treatment head.

1.7.5 Multileaf Collimators

Multileaf collimators (MLCs), as shown in Figure 1.28a, have replaced blocks for virtually all practical applications, and all new linacs are installed with an MLC attached. Each MLC device consists of a set of movable interleaved collimators.

Most MLC leaves are capable of driving several centimeters beyond the geometric center of the field (leaf overtravel). Each leaf produces a jagged-shaped dose distribution at the field edge, as each leaf produces a nominal 0.5-wide shadow at isocenter.

Computer-controlled MLCs allow rapid and flexible field shaping without blocks by using leaves of tungsten that block the beam. There are typically 120 or more leaves to cover the whole photon radiation field. From a beam's-eye view perspective, they shape the beam into any irregular shape, thus blocking out normal tissue structures. The leaves, usually made from machined tungsten, travel in two banks as opposing pairs. Each leaf is usually driven by a small rotating electric motor connected to a thread or some other precision-drive device. Precise leaf position feedback is important when blocking the field edge, and this becomes even more important when in-field segmentation is employed. MLCs have typical dose leakage values of 1%, with an extra 0.5% leakage between the leaves.

Different manufacturers employ different MLC designs and positions within the linac treatment head.

The Elekta Agility™ 160 leaf MLC, as shown in Figure 1.20a, is mounted closer to the target than the Varian design. The Elekta MLC is mounted above the two sets of jaws. One jaw is thinner and acts more as an extra MLC end leaf leakage

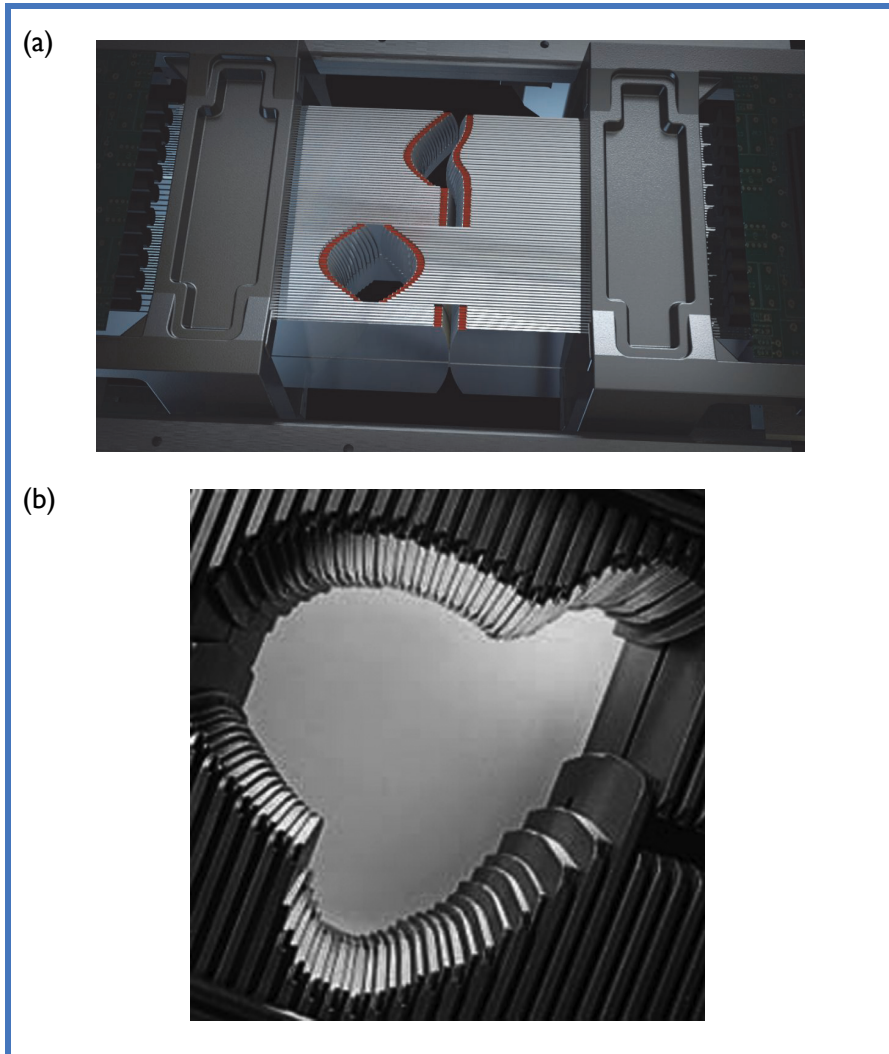


Figure 1.20 Multileaf collimators (MLCs). (a) Elekta Agility™ multileaf collimator. (Image courtesy of Elekta.) (b) Varian Millennium™ 120-leaf multileaf collimator. (Image courtesy of Varian Medical Systems, Inc. All rights reserved.)

attenuator. Leaf width at isocenter is also 0.5 cm. The Elekta MLCs also employ a single-focused design with a rounded leaf end.

There is more clearance between the linac treatment head and the patient with the Elekta MLC design, which is closer to the target. However, due to beam divergence this positioning causes greater magnification of MLC width at isocenter, so they need to have narrower physical leaf widths in their mounted position because they are mounted closer to the target. Most MLCs provide leaf widths that are 0.5 cm at isocenter.

The Varian open gantry linacs retain two sets of jaws, so the MLC is a tertiary collimator. A close-up of the Varian Millennium™ MLC is shown in Figure 1.20b. This design has 60 pairs of leaves, i.e., 120 leaves in total, which are affixed to the

machine just beyond the rectangular collimators and in front of the accessory holder. Most MLCs employ a single-focus leaf design. This means the leaf sides diverge to align with beam divergence in their cross-axis dimension. But because the leaves drive horizontally using a threaded screw design, a rounded leaf end is used to account for beam divergence in the other dimension. For the millennium, MLC leaf width at isocenter is 0.5 cm out to the $20 \times 20 \text{ cm}^2$ field size, then 1-cm leaves from 20 to 40 cm^2 field size. Varian also provides a high-definition MLC with some central leaf widths being 2.5 mm at isocenter. This option comes with a slightly reduced maximum field size.

Some exciting new designs employ dual leaf banks that do not require collimators. For example, the Varian Halcyon/Ethos linac employs a dual-bank design. The leaf banks are offset by half a leaf width, ensuring higher resolution leaf patterns, and the upper and lower banks replace the need for collimators. The multileaf collimators deployed in the ViewRay MRIdian™ MRI-linac has dual banks and a dual-focused design to provide alignment with beam divergence in both axes for a very sharp beam penumbra.

1.8 Wedges

1.8.1 Physical Wedges

Wedges are variable-thickness absorbers that are placed in the beam and cause a progressive decrease in dose intensity across the beam, resulting in tilted dose profiles. They are designed to give an angled isodose curve at a 10-cm reference depth. For example, a set of physical wedges generally allow 15-, 30-, 45-, and 60-degree angled isodose curves at a 10-cm depth. Physical wedges are generally made from brass, lead, or steel and are used at a distance from the source of about 40 cm. The effect of a wedge on the dose profile is shown in Figure 1.21a.

The introduction of a wedge produces a reduction in beam transmission (attenuation). This is accounted for by using wedge transmission factors to correct the dose delivered when a wedge is introduced into the x-ray beam. Because physical wedges attenuate low-energy photons, the beam is slightly harder than the open

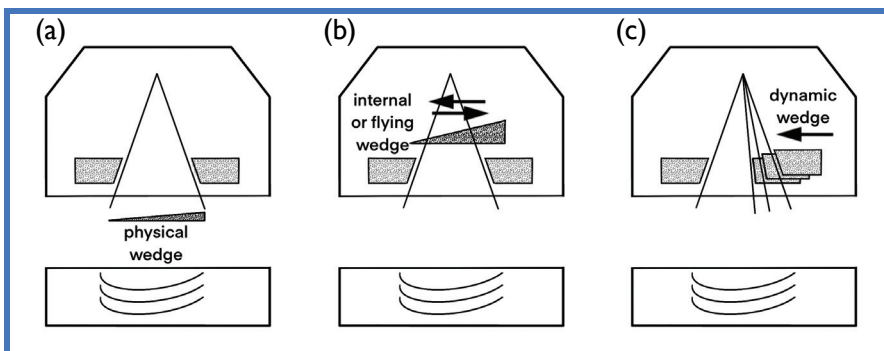


Figure 1.21 Different ways of providing a wedge-shaped dose distribution. (a) Physical wedge. (b) Flying wedge. (c) Dynamic wedge.

field. This results in depth dose curves for wedge fields being slightly shallower at depth. However, this effect tends to be very small, e.g., less than 2% difference for 6-MV linacs at a 30-cm depth. This effect does require separate central axis depth dose collection and input for modeling in radiation therapy treatment planning computers.

1.8.2 Flying Wedges

One manufacturer, Elekta, uses a steep physical wedge driven into the field for part of the treatment, sometimes called a *flying wedge*. These wedges are generally mounted internally in the gantry and are sometimes referred to as *internal wedges*. The dynamic movement of these devices produces resultant dose distributions that are the same as those made by a physical fixed wedge. The final dose distribution is determined by how long the wedge is retained in the beam relative to the open beam. Therefore, a multiple number of beam wedge angles can be created by the use of this single wedge. For example, if the wedge is 60 degrees and maintained in the field for a short time, with the rest of the dose delivered as an open field, the resultant wedge-shaped dose distribution will be some angle between 0 and 60 degrees (see Figure 1.21b).

1.8.3 Dynamic Wedges

The other two linac vendors, Varian and Siemens, employ dynamic wedges (Kijewski et al. 1978; Levitt et al. 1990). This is actually a dynamic jaw that sweeps across the beam to produce a dose distribution that is similar to a physical wedge's dose distribution (see Figure 1.21c). Unlike physical and flying wedges, there is no apparent beam hardening when dynamic wedges are employed, so the central axis depth dose for an open field is the same as for a dynamic wedge field of the same dimensions.

Any number of wedge angles are potentially available without physical wedge placement. The angles are not restricted, but in the interests of data collection efficiency, the wedge angles commonly released for dynamic wedges are 10, 15, 20, 25, 30, 45, and 60 degrees.

Using a similar principle to the flying wedge, dynamic wedges have the jaws open, and a large proportion of the dose is given as a flat dose profile. Then the jaws are closed or opened at progressive intervals during which time a different preset dose is given. The preset dose per interval is obtained from a look-up table and is sufficient at each interval to give the steepest-angled dose distribution available (i.e., 60 degrees). Then the other wedged angles are simply provided by altering the weight of the open field component of the beam relative to the weight of the steep wedged dose component of the beam.

1.9 Image Guidance Devices

1.9.1 Electronic Portal Imaging Devices

The *electronic portal imaging device* (EPID) consists of an amorphous silicon plate detector array placed on the opposite side of the rotating gantry from the treatment beam portal. The EPID is mounted on a retractable arm (see Figure 1.22) and is designed to replace the historical method of treatment position validation, which



Figure 1.22 Electronic portal imaging device (EPID) on a Varian TrueBeam® mounted on a robotic arm so that the device can be retracted away during routine treatment or extended out for an MV image. (Image courtesy of Varian Medical Systems, Inc. All rights reserved.)

was to place a film in this position (known as a *port film*). Most EPIDs consist of an amorphous silicon (a-Si) detector array overlaid with a fluorescent layer, usually gadolinium oxysulphide (GdOS) or cesium iodide (CsI).

Because the EPID image is produced using megavoltage (MV) beam energy, the image does not have as much contrast resolution as simulator images (diagnostic tube). Sufficient bony landmark anatomy may be visible to enable an alignment comparison between EPID images and simulator images or, indeed, *digitally reconstructed radiographs* (DRRs), which are images reconstructed from CT data.

1.9.2 On-Board kV Imaging and Cone-Beam CT

Varian calls their kV device an *on-board imager* (OBI), which consists of a diagnostic kilovoltage (kV) x-ray tube and a *flat-panel detector* (FPD) device capable of planar and cone-beam CT acquisition. As with an EPID, the FPD usually consists of an a-Si detector array and a fluorescent layer. The OBI is placed on the linac gantry at 90 degrees to the linac treatment head. Elekta refers to their device directly as a cone-beam CT imager, as shown in Figure 1.23. For both vendors, the x-ray tube and FPD are mounted on retractable arms and can be deployed when a high-quality image of patient position is required. Both can provide fixed beam's-eye view-type orthogonal x-ray images or can be rotated around the patient to provide cone-beam CT images of patient anatomy.



Figure 1.23 Cone-beam CT device including kV x-ray tube and flat-panel imager mounted at 90 degrees to linac treatment head mounted on an Elekta Versa HD™. (Image courtesy Elekta.)

1.10 Innovative Linac Machines

1.10.1 Helical Tomotherapy-Radixact®

First proposed by Mackie et al. (1993), helical tomotherapy linacs employ a single-energy, in-line waveguide with fixed target and flattening filter free linear accelerator. All ancillary equipment, including the modulator, is mounted on a closed CT-type slip ring gantry, as shown in Figure 1.24. A fan-beam treatment is delivered continuously during the 360-degree gantry rotation. Beam modulation is achieved using a pneumatically driven binary MLC. Modulation in the superior-inferior dimension is also achieved by delivering the treatment using helical treatment delivery, as the patient treatment couch moves through the gantry. Variable combinations of gantry rotation speed and table drive speed provide different pitches at which the treatment can be delivered. By reducing the delivery pitch, beam modulation in a patient's superior-inferior dimension produces extremely fine resolution.

1.10.2 Halcyon-Ethos

The Varian Halcyon-Ethos linac consists of a closed-gantry linac, as shown in Figure 1.25. It also employs an in-line 6-MV linac in an enclosed cone-beam device. While not employing a slip ring, it can rotate several rotations in one direction. Any closed-gantry linac has the advantage that it can rotate faster than one revolution per minute, which is a safety limit imposed on open-gantry linacs. This linac has a fixed target, is flattening filter free, and has a dual-bank multileaf collimator. The Ethos version of this machine places an emphasis on being able to replan treatments using cone-beam images acquired and then providing an adaptive treatment.



Figure 1.24 Radixact® Tomotherapy linac mounted on a closed gantry using helical delivery and pneumatic-driven binary multileaf collimators. (Image used with permission from Accuray Incorporated.)

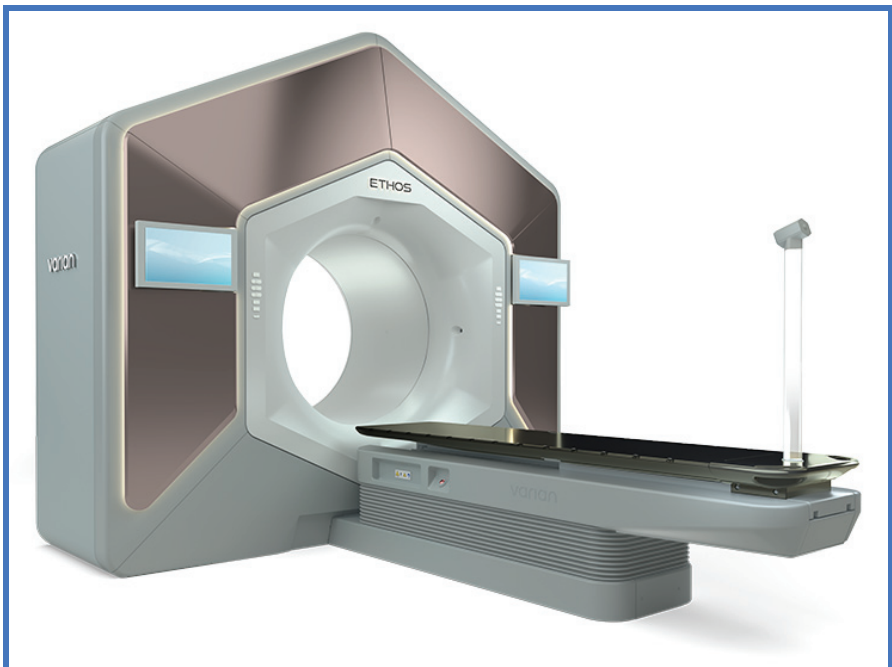


Figure 1.25 Varian Ethos linac mounted on a closed gantry using dual-bank multileaf collimators. (Image courtesy of Varian Medical Systems, Inc. All rights reserved.)



Figure 1.26 External view of a CyberKnife[®], which is a linac mounted on a robotic arm that incorporates 2D stereoscopic x-ray imaging and motion-adaptive treatments. (Image used with permission from Accuray Incorporated.)

1.10.3 CyberKnife[®]

The CyberKnife[®] is a linac mounted on a robotic arm that can produce radiotherapy x-ray beams from multiple noncoplanar directions (see Figure 1.26). The device can provide frameless stereotactic radiosurgery (SRS) using an image correlation algorithm for target localization (Adler et al. 1997). It is also used in combination with diagnostic x-ray tubes and flat-panel images in order to obtain frameless stereotactic images. This device was originally designed to compete with the Gamma Knife[®]. The Gamma Knife is an extremely precise multiple-source cobalt-60 machine that was first introduced in the 1960s. It continues to provide sub-millimeter cranial radiotherapy precision treatment for brain tumors, metastases, and, in particular, arteriovenous malformations (AVMs).

Due to the mobility provided by its robotic arm, CyberKnife is also being used in extra-cranial parts of the body due to its image-guidance capability. It has been used for tracking radiotherapy lung treatment by a combination of lung position prediction and tracking of *in situ* markers (Whyte et al. 2003). A review comparing three stereotactic radiosurgery systems—including Gamma Knife, CyberKnife, and the Novalis radiosurgery linac—has been reported by Andrews et al. (2006).

1.10.4 Hybrid MRI-Linac

The hybrid MRI-linac combines two technologies—an MRI scanner to precisely see tumors in real time and a linear accelerator that irradiates tumors with x-rays. In



Figure 1.27 Elekta Unity MRI-linac combining a 7-MV linac with 1.5-T MRI for image guidance. An extra mounted body coil is shown which is employed in combination with a gantry-mounted body coil to enhance image quality. (Image courtesy of Elekta.)

essence, MR image guidance enables high soft tissue contrast, no increased secondary cancer risk from imaging dose, and intra-fraction images. There may also be potential for biological analysis of tumor response using on-line perfusion imaging.

The ViewRay MRIdian 0.35-T MRI was originally combined with cobalt-60 and treated the first patients in 2014. These devices have been modified to MRI-linacs and have provided patient treatments since 2017 (Mutic and Demsey 2014). Another MRI-linac, the Elekta Unity 1.5-T 7-MV linac, provides a high magnetic field strength (Lagendijk et al. 2008; Lagendijk et al. 2014). The Elekta Unity device also started patient treatments in 2017 and is shown in Figure 1.27. Both linacs rotate around a fixed MRI gantry, so the x-ray treatment beam delivery is transverse to the magnetic field. This introduces some interactions between the Lorentz force of the B field and Compton-generated electrons, leading to interesting electron return effects (Oborn et al. 2010). There are currently about 70 MRI-linacs installed, with the number of machines increasing rapidly. A recent review of MRI-linacs and their real-time image guidance capabilities is given by Lagendijk et al. (2020).

This chapter outlined the basic physics principles of linac operational design. This chapter has also provided a taste of the exciting proliferation of innovative design for new linac beam delivery systems. Subsequent chapters will identify and explain these key innovations in more detail.

References

- Adler, J. R. Jr., S. D. Chang, M. J. Murphy, J. Doty, P. Geis, and S. L. Hancock (1997). "The CyberKnife: a frameless robotic system for radiotherapy." *Stereotact. Funct. Neurosurg.* 69(1–4 Pt2):124–28.
- Andrews, D. W., G. Bednarz, J. J. Evans, and B. Downes (2006). "A review of 3 current radiosurgery systems." *Surg. Neurol.* 66(6):559–64.
- Attun, R., D. A. Jaffray, M. B. Barton, F. Bray, et al. (2015). "Expanding global access to radiotherapy." *Lancet Oncol.* 16:1193–1224.
- Bekelman, J. E., A. Denicoff, and J. Buchsbaum (2018). "Randomized Trials of Proton Therapy: Why they are at risk, proposed solutions, and implications for evaluating advanced technologies to diagnose and treat cancer." *J. Clin. Oncol.* 38(24):2461–66.
- Einstein, A. (1905). "On the electrodynamics of moving bodies." *Ann. Physik.* 17:891.
- Greene, D. (1986). "Linear Accelerators for Radiation Therapy." *Medical Physics Handbook* 17. Bristol, UK: Adam Hilger.
- Ishikawa, H., H. Tsuji, T. Kamada, N. Hirasawa, T. Yanagi, J. E. Mizoe, K. Akakura, H. Suzuki, J. Shimazaki, and H. Tsujii (2006). "Risk factors of late rectal bleeding after carbon ion therapy for prostate cancer." *Int. J. Radiat. Oncol. Biol. Phys.* 66(4):1084–91.
- Johns, H. E. and J. R. Cunningham (1983). *The Physics of Radiology*, 4th Ed. Springfield, Illinois: Charles C. Thomas.
- Johns, H. E. and J. R. Cunningham (1959). "A precision cobalt-60 unit for fixed and rotational therapy." *Am. J. Roentgenol.* 81:4–6.
- Johns, H. E., S. O. Fedoru, R. O. Kornelson, E. R. Epp, and E. K. Darby (1952a). "Depth dose data, 150 kVp to 400 kVp." *Br. J. Radiol.* 25:542–49.
- Johns, H. E., E. R. Epp, D. V. Cormack, and S. O. Fedoruk (1952b). "1000 Curie cobalt units for radiation therapy." *Br. J. Radiol.* 25:296.
- Karzmark, C. J. and R. J. Morton (2017). *A Primer on the Theory and Operation of Linear Accelerators in Radiation Therapy*, 3rd Ed. Madison, WI: Medical Physics Publishing.
- Kijewski, P. K., L. M. Chin, and B. E. Bjarngard (1978). "Wedge-shaped dose distributions by computer-controlled collimator motion." *Med. Phys.* 5:426–29.
- Krieger, H. and W. Petzold (1989). *Strahlenphysik, Dosimetrie und Strahlenschutz*. Stuttgart, Germany: B.G. Teubner.
- Legendijk, J. and B. Raaymakers (2008). A MRI-linac integration. *Radiother. Oncol.* 86:25–29.
- Legendijk J., B. Raaymakers, and M. van Vulpen (2014). "The Magnetic Resonance Imaging-Linac." *Semin. Radiat. Oncol.* 24:207–09.
- Legendijk, J., B. Raaymakers, R. Tijssen, and B. van Asselen (2020). "Real-Time Image Guidance with Magnetic Resonance." In *The Modern Technology of Radiation Oncology: A Compendium for Medical Physicists and Radiation Oncologists*, Vol 4. J. Van Dyk, Ed. Madison, WI: Medical Physics Publishing.
- Levitt, D. D., M. Martin, J. H. Moeller, and W. L. Lee (1990). "Dynamic wedge field technique through computer-controlled collimator motion and dose delivery." *Med. Phys.* 17:87–91.
- Locke, J., S. Karimpour, G. Young, M. A. Locket, and C. A. Perez (2001). "Radiotherapy for Epithelial Skin Cancer." *Int. J. Radiat. Oncol. Biol. Phys.* 51(3):748–55.
- Mackie, T. R., T. Holmes, S. Swerdloff, P. Reckwerdt, J. O. Deasy, J. Yang, B. Paliwal, and T. Kinsella (1993). "Tomotherapy: a new concept for the delivery of dynamic conformal radiotherapy." *Med. Phys.* 20(6):1709–19.
- Mutic, S. and J. F. Dempsey (2014). "The ViewRay system: magnetic resonance-guided and controlled radiotherapy." *Semin. Radiat. Oncol.* 196–99.
- Oborn, B., P. E. Metcalfe, M. J. Butson, and A. B. Rosenfeld (2010). "Monte Carlo characterization of skin doses in 6MV transverse field MRI-linac systems: Effect of field size, surface orientation, magnetic field strength, and exit bolus." *Med. Phys.* 5208–17.
- Particle Therapy Co-operative Group (PTCOG) (2021). Available at <https://www.ptcog.ch/index.php/facilities-in-operation>.
- Podgorsak, E. B., J. Van Dyk, and P. Metcalfe (1999). "Linear accelerators." In *The Modern Technology of Radiation Oncology*. J. Van Dyk, Ed. Madison, WI: Medical Physics Publishing.
- Shipley, W. U., L. J. Verhey, J. E. Munzenrider, H. D. Suit, M. M. Urie, et al. (1995). "Advanced prostate cancer: the results of a randomized comparative trial of high dose irradiation boosting with conformal protons compared with conventional dose irradiation using photons alone." *Int. J. Radiat. Oncol. Biol. Phys.* 32(1):3–12.
- Thwaites, D. I. and J. B. Tuohy (2007). "Back to the future: the history and development of the first clinical linear accelerator." *Phys. Med Biol.* 51(13):R343–62.
- Whyte, R. I., R. Crownover, M. J. Murphy, D. P. Martin, T. W. Rice, et al. (2003). "Stereotactic radiosurgery for lung tumors: preliminary report of a phase I trial." *Ann. Thorac. Surg.* 75(4):1097–101.

Questions

- 1.1 Explain the main difference between traveling and standing waveguide accelerators. (See Section 1.5.)
- 1.2 Explain the main difference between a magnetron and a Klystron. (See Section 1.5.)
- 1.3 If a 6-MeV electron beam needs to travel in a radius of curvature of 15 cm to traverse around the bend magnet, what magnitude of magnetic field is required if one assumes a constant magnetic field? (See Section 1.6.)
- 1.4 Describe the main efficiency gain from multileaf collimators (MLCs) that lead to them replacing shielding blocks. (See Section 1.8.)
- 1.5 What are the practical advantages of using dynamic wedges instead of conventional wedges in combination with MLCs. Describe another way of using MLCs that negates the requirement for wedges. (See Section 1.8.)